| | |
|---|---|
| **Project** | AtlantOS – 633211 |
| **Deliverable number** | 3.5 |
| **Deliverable title** | Study of the potential for existing bathythermic string drifters |
| **Description** | Evaluation report on the use of subsurface temperature buoy data and on their ability to provide suitable measurements in the ocean boundary layer |
| **Work Package number** | 3 |
| **Work Package title** | Enhancement of autonomous observing networks |
| **Lead beneficiary** | CNRS |
| **Lead authors** | Pierre Rousselot and Gilles Reverdin (CNRS),<br>Pierre Blouch and Paul Poli (EUMETNET/Météo-France) |
| **Contributors** | Review by Felix Janssen (AWI) |
| **Submission data** | |
| **Due date** | April 2017 (PM 24) |
| **Comments** | |

This project has received funding from the European Union's Horizon 2020 research and innovation programme under grant agreement n° 633211.

Last updated: 29 March 2017

# Abstract

This report revisits data collected by thermistor chains on free-drifting buoys. These buoys have been mainly deployed in the 1980s-90s, with a decrease since the 2000s owing to the growth of ARGO profiler deployments but they are still used nowadays. Indeed, these buoys provide an interesting monitoring of the thermal structure of the oceanic superficial layers. They offer an intermediate vertical resolution between moored buoys and profiler instruments with a high temporal resolution. This high temporal resolution is particularly interesting because it allows a better filtering of the sampling errors and offers an accurate monitoring of the superficial layers variability. This study highlights two particular types of buoys that were the most used since the 2000's: the SVP-BTC, developed by the Marlin-Yug company, and the Marisonde, developed by Météo-France. The analysis is based upon the co-localization of nearby buoys, thermosalinograph data and ARGO and CTD profiles. These comparisons show systematic differences more particularly in surface and at mid-chain levels of the profiles. At the chain end and just below the surface, the biases are nearly non-existent. The important issue of these instruments resides in the fact that the chain behavior isn't controlled. Indeed, most of the buoys are equipped with only one pressure sensor at the end of the chain. A model must be applied to settle the sensors to their 'real' immersion when the bottom of the chain uplifts. Unfortunately, these models are empirical or based on experimental design and not optimal, so that important errors of immersion are found in the presence of strong subsurface currents. In this study, a new model is proposed and used resulting in biases that usually don't exceed 0,2°C. The reduced level of inaccuracy renders this kind of instruments an even more useful tool for surface ocean observation. Nevertheless, they are still in development and future buoys will get more pressure sensors, more ballast at the end of the chain and maybe more sensors to measure other physico-chemical parameters, such as salinity or dissolved oxygen.

# Table of Contents

# I. Introduction

Measuring physical parameters in the superficial layers of the ocean has always been an arduous task. Over the last decades, the quality of observations of the ocean surface has greatly improved, but regular data coverage at fixed locations remains scarce (i.e., CTD, XBT, and moored buoys), and do not allow to monitor satisfactorily the spatio-temporal evolution.

It is yet at the surface that key processes influencing the ocean and atmospheric circulation and mixing processes in the euphotic zone are taking place. Satellites only observe the very surface, and cannot probe through it (even if inverse methods can be applied to infer some bulk properties about the entire ocean column). Consequently, it is only by better observing the upper ocean layers that one may eventually improve models and prediction.

Argo floats and drifting buoys with bathythermic strings are able to sample the upper ocean layers, though at differing time intervals (10- or 15-day cycles for floats, which furthermore typically stop a few meters below the surface to prevent biofouling).

Bathythermic string drifters were first tried in the early 1980s, before profiling floats were invented. However, the bathythermic string drifters still offer the possibility of sampling several times per day the ocean upper layers.

# II. State-of-the-art

Various types of bathythermic string drifters have been developed over the past 30 years. In general, they all measure atmospheric pressure, barometric tendency, subsurface temperature at various depths, and hydrostatic pressure at the bottom of the string or chain (plus internal parameters, such as battery voltage).

The data are collected in near-real-time via satellite communication, and the lifetimes vary from one month to one year.

This report first reviews the various types of buoys that were developed, and then puts an

emphasis on two particular bathythermic string drifters: the Surface Velocity Program drifter with Barometer and Thermistor Chain (**SVP-BTC)**, developed by company Marlin-Yug, and the **Marisonde**, developed by Météo-France.

## A review of the bathythermic string drifters

Below is a consolidated list of bathythermic string drifters, from the majority of platforms of such type that have been deployed and documented:

- The BODEGA buoy (du Penhoat et al., 1995): the floats were manufactured by the company SERPE-IESM (now part of the company NKE). These buoys use 5 thermistors sampling depth down to 20 m. Implementation occurred in the Pacific Ocean at the end of the 1980s and the beginning of the 1990s by the Laboratoire d'Océanographie Dynamique et de Climatologie (LODYC -- now called Laboratoire d'Océanographie et du Climat: Expérimentations et Approches Numériques, LOCEAN). They are close in design to the SVP-BTC, allowing to sample the diurnal cycle.
- The Compact Meteorological and Oceanographic Drifter (CMOD) buoy (also referred to as XAN-3): the floats are manufactured by the company Metocean. These buoys have been used mainly by NATO countries (e.g., Mariette et al., 2002) and can be air-dropped (a parachute preventing damage). The buoy self-inflated upon touching the surface, and the bathythermic string was dropped at the same time. A hydrostatic pressure sensor was employed to monitor the string shape.
- The NKE SC-40 TPI buoy: the floats are manufactured by the company NKE. They have been used by SHOM. The data are transmitted to the buoy by induction. They are available in two lengths: 120 m depth, and 200 m depth. Both models use 4 hydrostatic pressure sensors along the chain. Furthermore, a deadweight is at the bottom.

There may have been more model types, but no significant documentation was found. Two other models for which data were easily accessible in the CORIOLIS database are now discussed in more details.

## The SVP-BTC buoy

The SVP-BTC is derived from the SVP of the Global Drifter Program, initially designed in the 1980s, initially solely to track ocean surface currents at a depth of 15 m and measure sea-surface temperature. Figure 1 shows a schematic of such buoys. The floats have a diameter around 40 cm. The ability to measure air pressure was added in the 1990s (SVP-B buoy), and other drifters were developed to monitor also sea-surface salinity (SVP-S), or a combination of the two (SVP-BS). A leading manufacturer of SVP-BTC buoys is the company Marlin-Yug based in the Russian Federation, at time of writing.

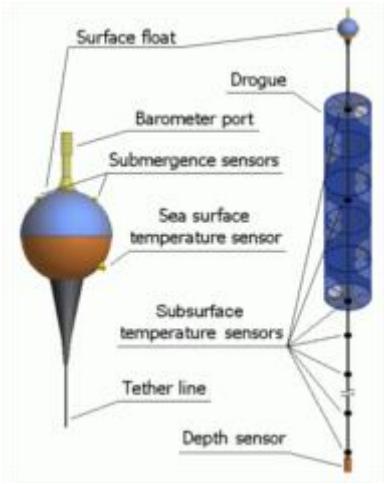


**Figure 1: Sketch of a SVP-BTC drifting buoy (Credits: Marlin-Yug)**

Most SVP-BTC developed so far include 80 meter-long chains, and use Dallas semiconductor thermal sensors. The buoy also includes a holey drogue sock to track currents. A similar type of buoy is the UpTempO buoy used by University of Washington in the polar regions, except the string goes through the sea-ice.

Data from SVP-BTC require processing before analysis. The depth of the bottom of the chain is first computed from the pressure measured there assuming freshwater density (at 1000 kg/m$^3$) at air pressure of 1000 hPa. To correct for actual water density ($\rho_{new}$) and air pressure ($P_{BP}$), the following equation is employed to derive an improved depth ($H_{new}$):

$$H_{new} = \frac{1000}{\rho_{new}}(H_{old} + 10.2) - \frac{P_{BP}}{g.\rho_{new}}$$

This only informs about the bottom of the string and does not give a complete information

about the string shape. To do this, a string shape (including inclination) model is generally applied.

## The Marisonde buoy

The Marisonde buoy was developed on the basis of the first drifting buoys, the FGGE buoys. It measures temperature at depths that differ from the SVP-BTC (Table 1).

| | SST | 0.5m | 1m | 5m | 7,5m | 10m | 12m | 12.5 | 15m | 17,5 | 20m | 25m |
|---|---|---|---|---|---|---|---|---|---|---|---|---|
| SVP | X | | | | | X | X | | X | | X | X |
| Marisonde1 (150m) | X | | | | | | | | X | | | |
| Marisonde2 (200m) | X | | | | | | | | | | X | |
| Marisonde3 (300m) | X | X | | X | X | | | X | | X | | X |
| PIRATA ATLAS | | X | | | | | | | | | X | |
| PIRATA T-FLEX | | | X | X | | X | | | | | X | |
| TAO | | | X | | | X | | | | | | X |

| | 30m | 32,5 | 35m | 40m | 45m | 50m | 55m | 60m | 65m | 70m | 75m | 80m | 90m |
|---|---|---|---|---|---|---|---|---|---|---|---|---|---|
| SVP | X | | X | X | X | X | X | X | X | X | X | X | |
| Marisonde1 (150m) | X | | | | X | | | X | | | X | | X |
| Marisonde2 (200m) | | | | X | | | | X | | | | X | |
| Marisonde3 (300m) | | X | | X | | X | | | | | X | | |
| PIRATA ATLAS | | | | X | | | | X | | | | X | |
| PIRATA T-FLEX | | | | X | | | | X | | | | X | |
| TAO | | | X | | X | | | | | | | X | |

| | 100m | 105m | 120m | 135m | 140m | 150m | 160m | 180m | 200m | 220m | 250m | 260m | 300m |
|---|---|---|---|---|---|---|---|---|---|---|---|---|---|
| SVP | | | | | | | | | | | | | |
| Marisonde1 (150m) | | X | X | X | | X | | | | | | | |
| Marisonde2 (200m) | X | | X | | X | | X | X | X | | | | |

**Table 1: Distribution of the temperature sensors along the bathythermic string for various kinds of drifting and moored buoys [red indicates the bottom of the string].**

The float of the Marisonde buoy is a profiled mast, up to 4 m height, and with a diameter around 80 cm (Figure 2). A deadweight of 25 kg is used to give the string some rigidity, with the aim to keep it as vertical as possible. The holey sock drogue is then distinct from the bathythermic string.


**Figure 2: Marisonde buoy (Credits: Météo-France).**

The first Marisonde buoy did not measure wind but this was quickly added. Various lengths of strings were tried, reaching 300 m in the last version. A particular difficulty with these buoys is their use of multiple Argos messages for a single transmission, requiring a complex post-analysis operation so as to reconstruct complete observation messages. There are no plans at present to upgrade these equipments to use Iridium transmission as used by SVP-BTC.

Table 2 below shows a comparison of SVP-BTC and Marisonde buoy specifications. Costs cannot be compared, as SVP-BTC are standard industrial products, whereas Marisonde buoys are homegrown developments which cannot be easily replicated.

| | SVP-BTC | Marisonde |
|---|---|---|
| Hydrostatic Pressure | Range : 0 to 250 m<br>Resolution : 1 m<br>Accuracy : ± 1 m | Range: 0 to 50 bar<br>Resolution: 0.02 bar<br>Accuracy: --- |
| Sea-surface temperature | Range: -5 to 35.88°C<br>Resolution: 0.08°C<br>Accuracy: ± 0.1°C | Range: -9.5 to 41.5°C<br>Resolution: 0.012°C<br>Accuracy: 0.05°C |
| Subsurface temperature | Range: -5 to 35.92°C<br>Resolution: 0.04°C<br>Accuracy: ± 0.1°C | Range: -9.5 to 41.5°C<br>Resolution: 0.012°C<br>Accuracy: 0.05°C |

**Table 2: Specifications of the sensors on SVP-BTC and Marisonde drifting buoys.**

## III. Data quality assessment

The bathythermic string drifters offer a greater vertical resolution than other comparable measurements from moored buoys, as shown in Figure 3 for example, considering one day worth of data from a PIRATA T-FLEX (latest generation) moored buoy and a nearby (within 10 km distance) SVP-BTC.

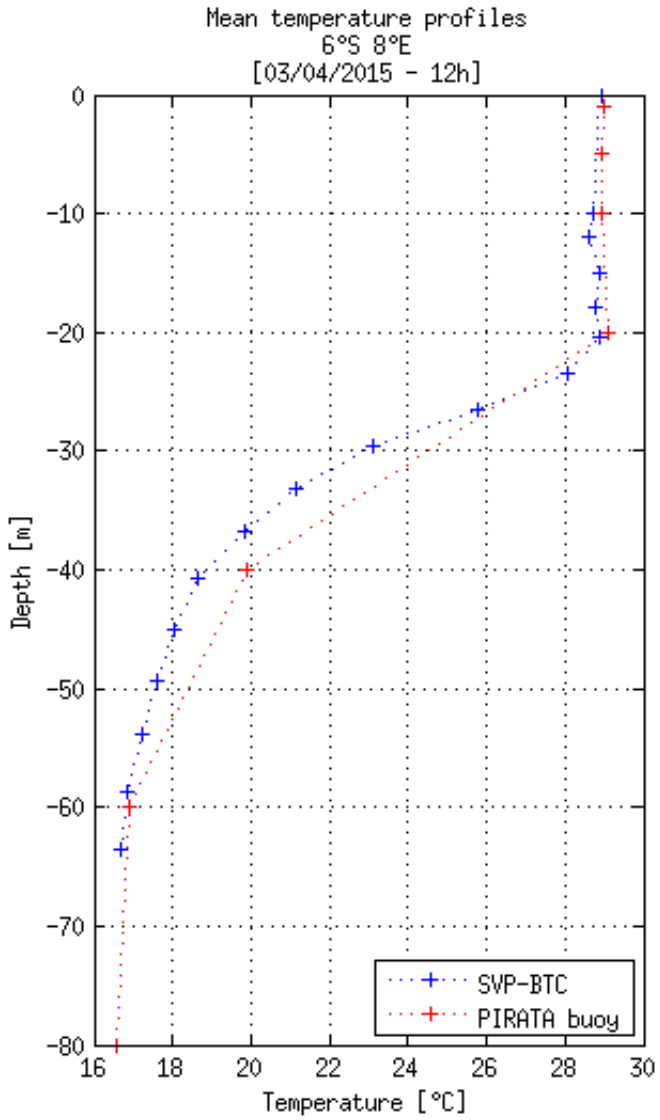


**Figure 3: Comparison of the vertical resolution of a drifting buoy SVP-BTC [WMO number 15953] with that of a moored buoy PIRATA.**

The bathythermic string drifters also offer a greater temporal resolution. Figure 4 shows an illustration over a month worth of data.

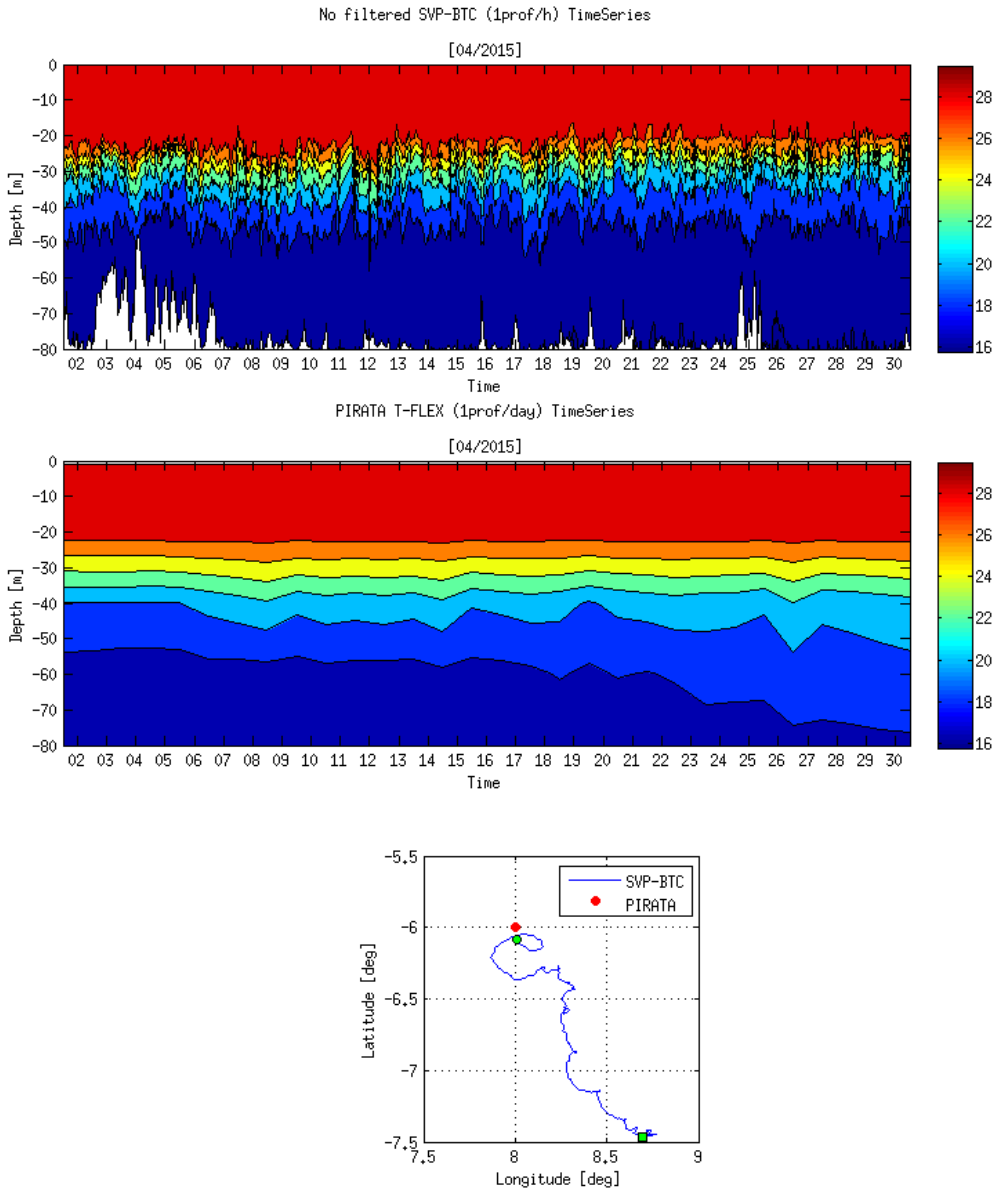


**Figure 4: Timeseries from a PIRATA T-FLEX moored buoy [located 6°S, 8°E, reporting 1 profile per day) and a nearby drifting buoy SVP-BTC [WMO number 15953, reporting 1 profile per hour]. Green circles (squares) indicate start (end, respectively) points.**

In parallel, this higher temporal resolution allows to apply filters that can extract more useful information from the SVP-BTC. This is illustrated with Figure 5 and Figure 6. Internal waves can be found near the thermocline, as well as tide signals or thermal fronts. However, note that moorings are increasingly upgraded to report hourly data.

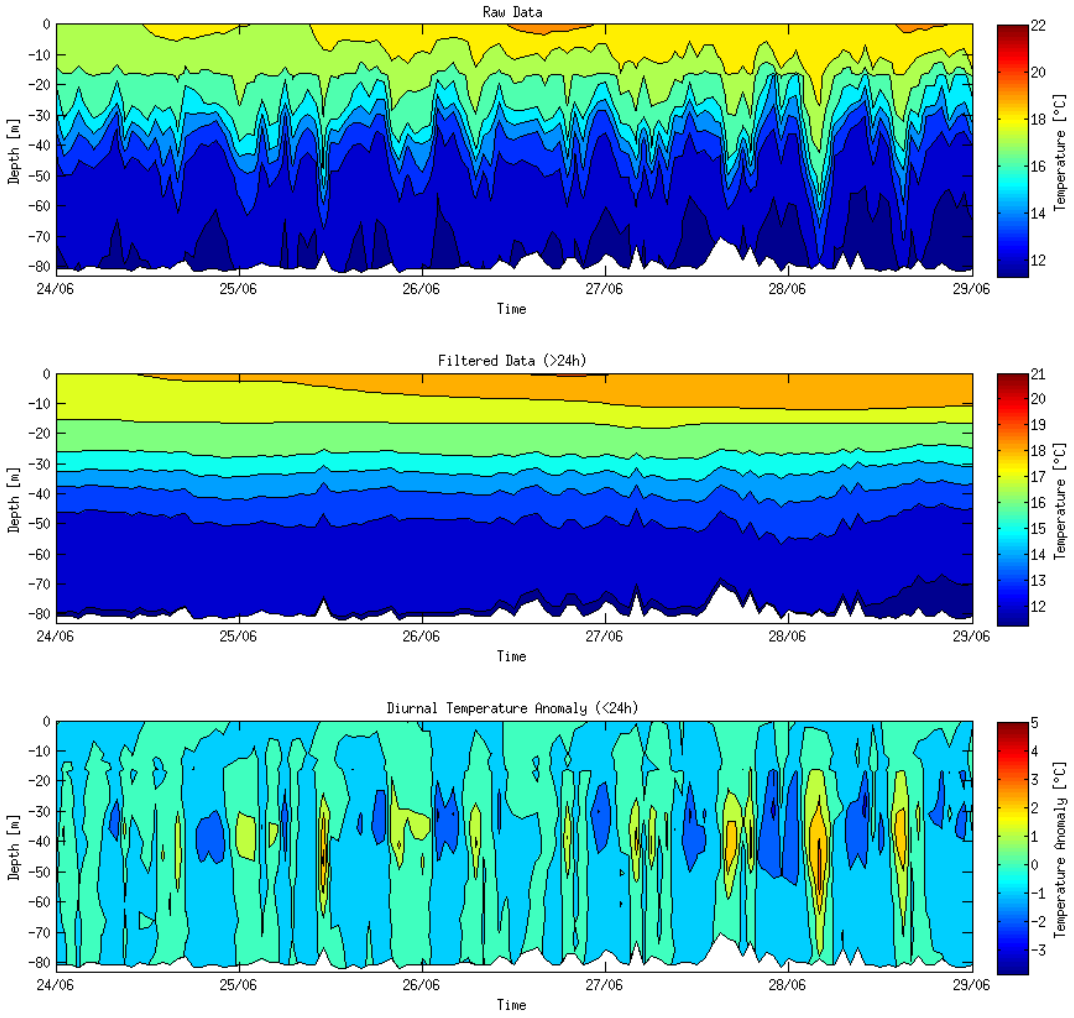


**Figure 5: (Top) Temperature oscillations in the Bay of Biscay measured by a drifting buoy SVP-BTC [June 2010, WMO number 62510]. (Middle) Low-frequency variability by application of a spectral filter [fft_filter]. (Bottom) High-frequency variability [diurnal temperature anomalies] by application of a spectral filter [fft_filter].**

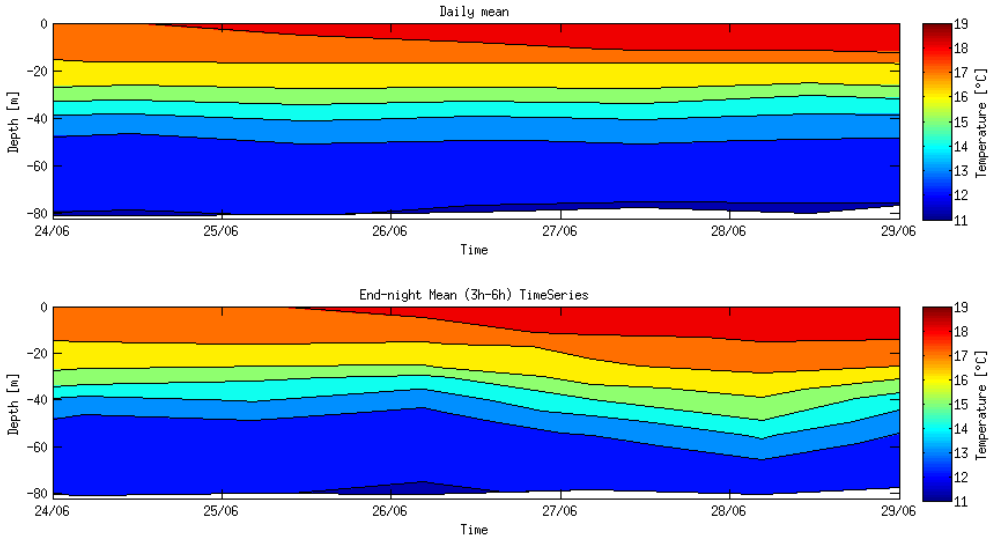


**Figure 6: Timeseries in the Bay of Biscay measured by a drifting buoy SVP-BTC [June 2010, WMO number 62510], showing (Top) daily averages and (Bottom) averages before dawn [between 3 hours and 6 hours].**

Retaining only data before dawn (between 03:00 and 06:00), more variations can be seen than by considering only daily averages. This is visible in Figure 7.

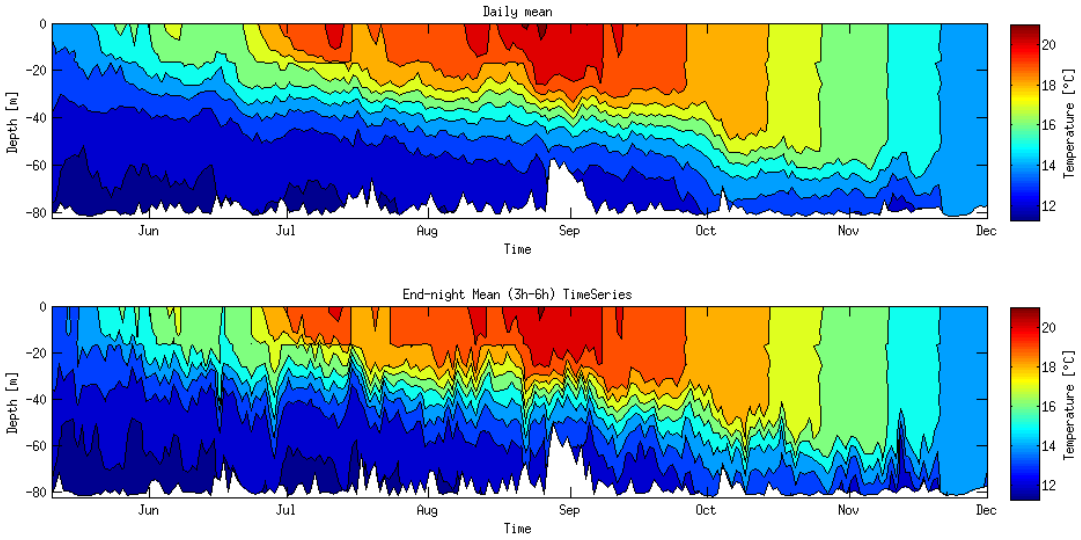


**Figure 7: Timeseries in the Bay of Biscay measured by a drifting buoy SVP-BTC [from May to December 2010, WMO number 62510], showing (Top) daily averages and (Bottom) averages before dawn [between 3 hours and 6 hours].**

## Comparing SVP-BTC and Marisonde

Data sampled by both types of buoys are compared in Figure 8.

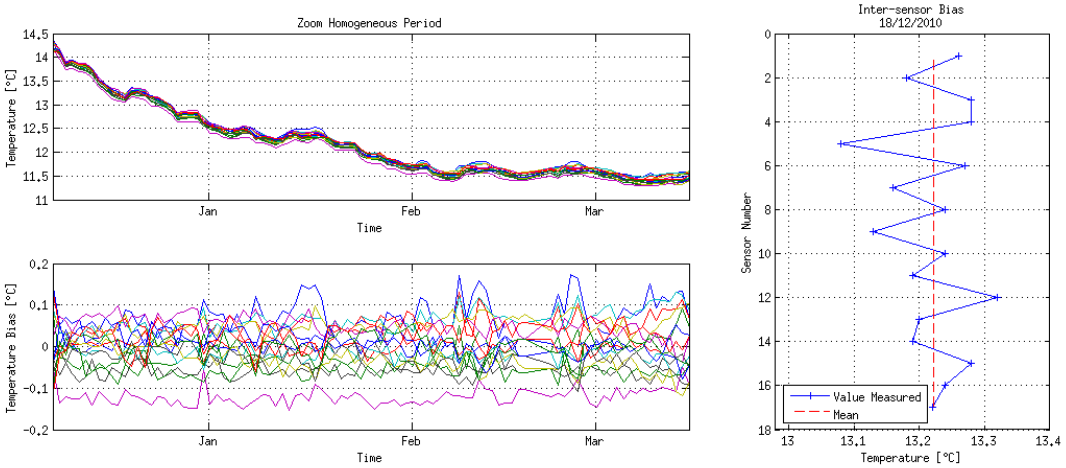


**Figure 8: Assessment of inter-sensor biases along the thermistor chain from a drifting buoy SVP-BTC [WMO number 62510] during transit in well-mixed waters [Bay of Biscay, Winter 2010/2011]. (Top left) Timeseries during transit in well-mixed waters. (Bottom left) Timeseries of departures from the all-sensor average (Right) Profile of departures on 18/12/2010 [red shows average].**

Table 3 shows that for both buoys, the sensor biases appear to be random and within specifications, except for the 5$^{th}$ sensor of the SVP-BTC, which seems to suffer from a calibration problem. Such problems are generally corrected by post-calibration of the sensors and correction of the data. Note the Marisonde data found in the CORIOLIS database do not always reflect the latest post-calibration.

| | SVP-BTC | | Marisonde | |
|---|---|---|---|---|
| Sensor no. | Average difference (x – μ) [general trend (January 2011)] | Std. Dev. | Average difference (x – μ) [general trend (March 2013)] | Std. Dev. |
| 1 | 0,072 [-0,023] | 0,034 | -0,036 [+0,05] | 0,045 |
| 2 | -0,024 [+0,002] | 0,015 | -0,009 [+0,071] | 0,043 |
| 3 | 0,040 [-0,012] | 0,017 | -0,004 [+0,074] | 0,042 |
| 4 | 0,054 [+0,008] | 0,016 | -0,001 [+0,05] | 0,039 |
| 5 | -0,127 [-0.001] | 0,015 | 0,017 [+0,035] | 0,035 |
| 6 | 0,047 [-0,004] | 0,016 | 0,007 [+0,027] | 0,037 |
| 7 | -0,059 [+0.001] | 0,014 | -0,003 [+0,017] | 0,028 |
| 8 | 0,005 [+0,003] | 0,012 | -0,017 [+0,002] | 0,02 |
| 9 | -0,055 [+0,008] | 0,015 | 0,005 [-0,001] | 0,02 |
| 10 | 0 [-0,005] | 0,017 | 0,011 [+0,001] | 0,027 |
| 11 | -0,018 [0] | 0,014 | 0,013 [-0,01] | 0,029 |
| 12 | 0,055 [-0,033] | 0,019 | -0,019 [-0,02] | 0,027 |
| 13 | -0,036 [-0,007] | 0,018 | 0,023 [-0,044] | 0,037 |
| 14 | -0,022 [-0,004] | 0,023 | 0,034 [-0,065] | 0,046 |
| 15 | 0,025 [-0,029] | 0,019 | -0,049 [-0,055] | 0,045 |
| 16 | 0,009 [+0,045] | 0,029 | 0,019 [-0,053] | 0,043 |
| 17 | 0,034 [+0,05] | 0,033 | 0,007 [-0,079] | 0,045 |

**Table 3: Inter-sensor bias assessment [plus trends over the month] for a drifting buoy SVP-BTC [WMO number 62510] and a Marisonde [WMO number 30837]. All data collected in well-mixed waters before dawn [between 3h and 6h].**

Figure 9 shows the tracks of nearby buoys in the framework of the HyMEX experiment, initially located within 3.2 miles of one another (at a time difference of 4 hours). They follow distinctly different paths. More important is the shapes of the paths, suggesting the two buoy types interact differently with the ocean currents. The string of the Marisonde buoy absorbs the high frequencies, and seems to reflect underlying ocean currents, whereas the SVP-BTC seems to represent better the ocean surface currents. Note the positions of the Marisonde suffer from inaccuracies related to the use of Argos for positioning (and data transmission), whereas the SVP-BTC uses GPS (and Iridium for data transmission).

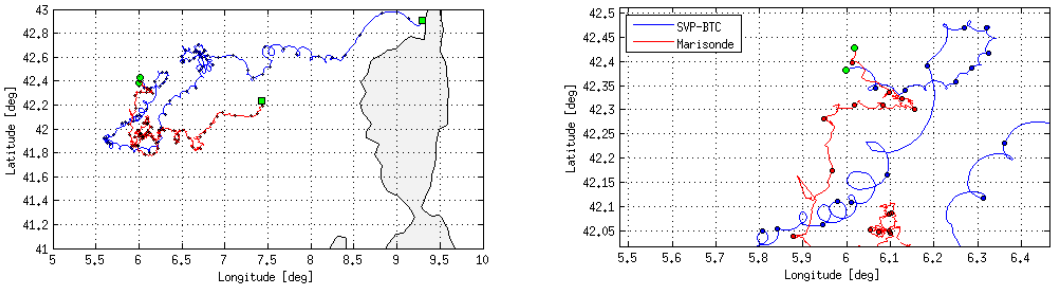


**Figure 9: Track of drifting buoys SVP-BTC and Marisonde between 04/09/2012 at 14h and 09/11/2012 at 19h, deployed in the framework of the HyMEX experiment [Green circles (squares) show start (end, respectively) points, and red and green circles show intermediate positions at 00:00].**

Figure 10 (Figure 11) shows the spatial (temporal, respectively) distributions of buoys that are used in a comparison thereafter, between September 2012 and March 2013. These pairs of buoys were selected because they remain within 6 miles of separation distance. In the temporal domain, only matching time reports are considered.

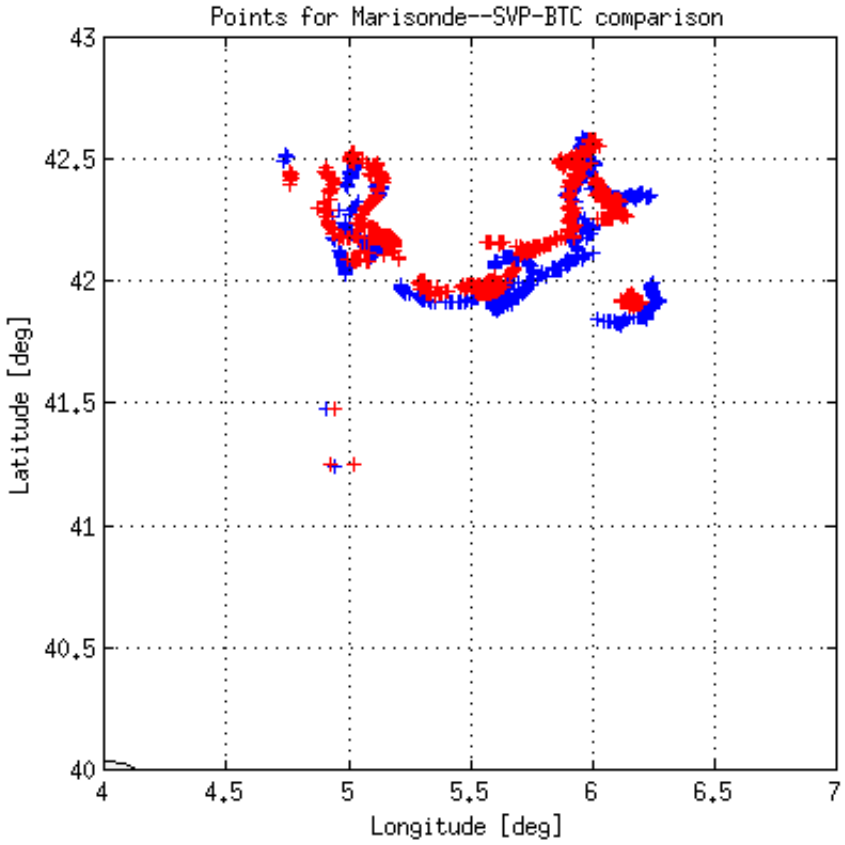


**Figure 10: Spatial distribution of the Marisonde and SVP-BTC buoys used in the comparison.**

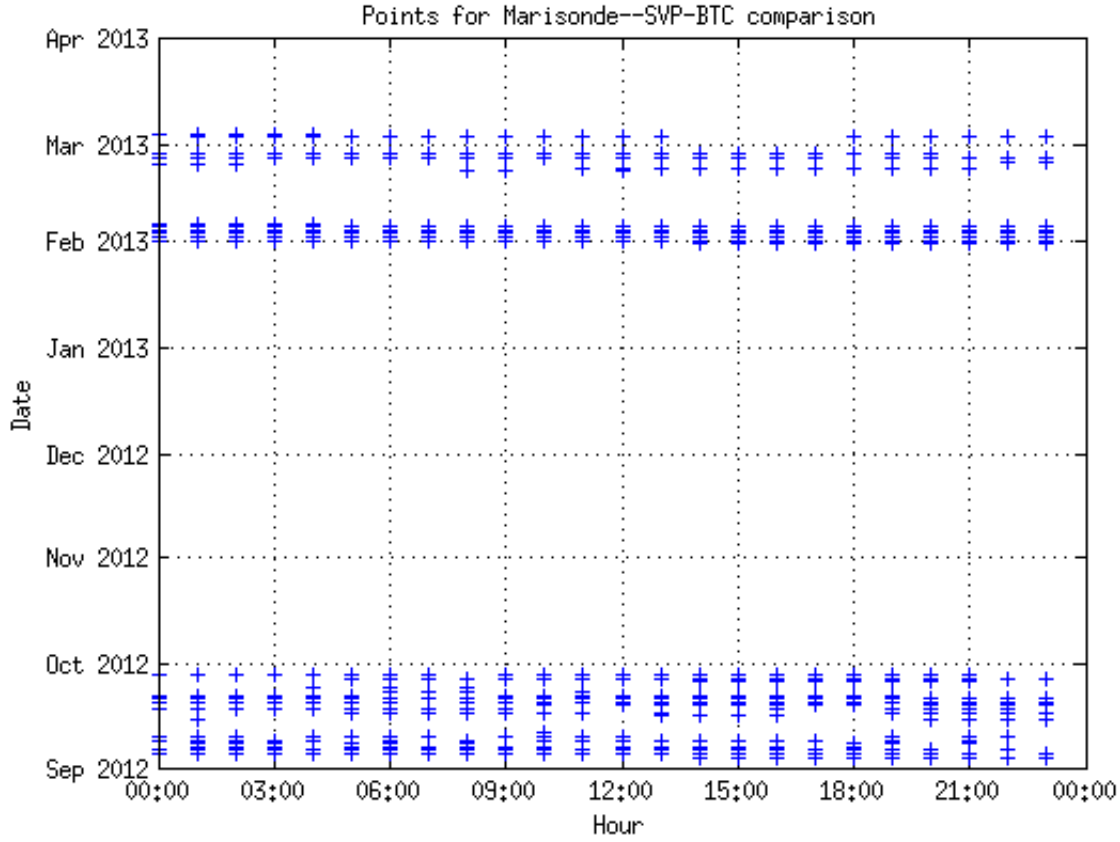


**Figure 11: Timeline of the Marisonde and SVP-BTC drifting buoys used in the comparison.**

For this comparison, only data at matching depths are considered, to avoid aliasing differences that come from different heights and could be due to propagating internal waves. All these comparisons consider the differences Marisonde minus SVP-BTC. Figure 12 shows histograms of differences.

At the surface, the modes of the histograms are highly biased, in contrast to subsurface temperature differences. In terms of spread, the distributions are more narrow at the surface and deeper down (50 m and 75 m depths), with standard deviations smaller than 0.5 K. At 25 m are the highest departures, with a standard deviation around 1 K, and 26% of the differences greater than 0.5 K.

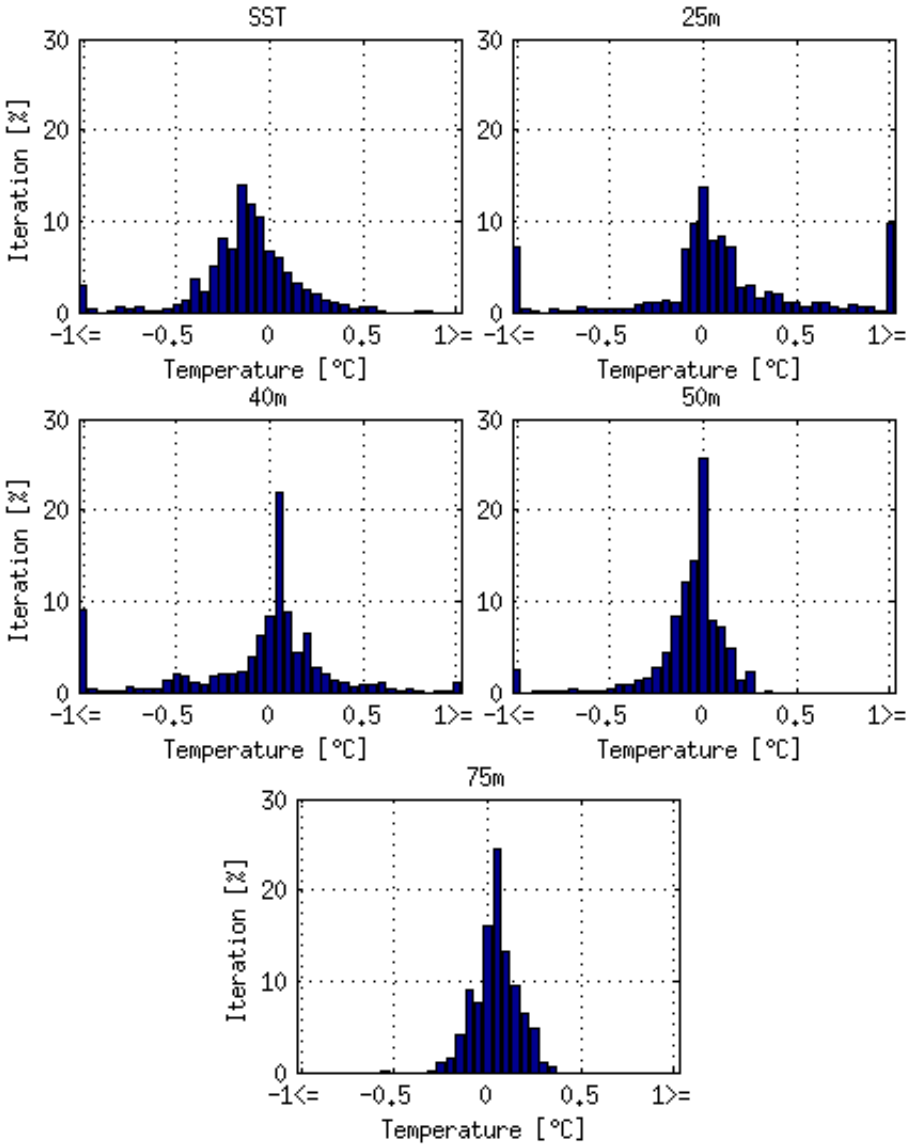


**Figure 12: Temperature differences at equivalent depths between measurements by Marisonde and by SVP-BTC [Marisonde minus SVP-BTC], at the same times, for buoys located nearby [within 6 miles separation distance, amounting to 867 comparisons during HyMEX].**

At the surface, the differences may be related to local (small gyre) effects, but also to differing reactions of the platforms to solar radiation. Indeed, the Marisonde sensors seem to under-estimate the surface temperatures with respect to the SVP-BTC. Note that Marlin-Yug now uses white floats to minimize the solar heating of the sensors. Figure 13 confirms this hypothesis by only considering differences before dawn (between 00:00 and 07:00), when temperatures are the most stable. The figure also shows differences during the maximum of solar heating (between 08:00 and 15:00). During night-time (day-time), 99% (83%) of the differences are smaller than 0.5 K. This would confirm the hypothesis that the sensors on Marisonde and on SVP-BTC react differently to solar

heating.

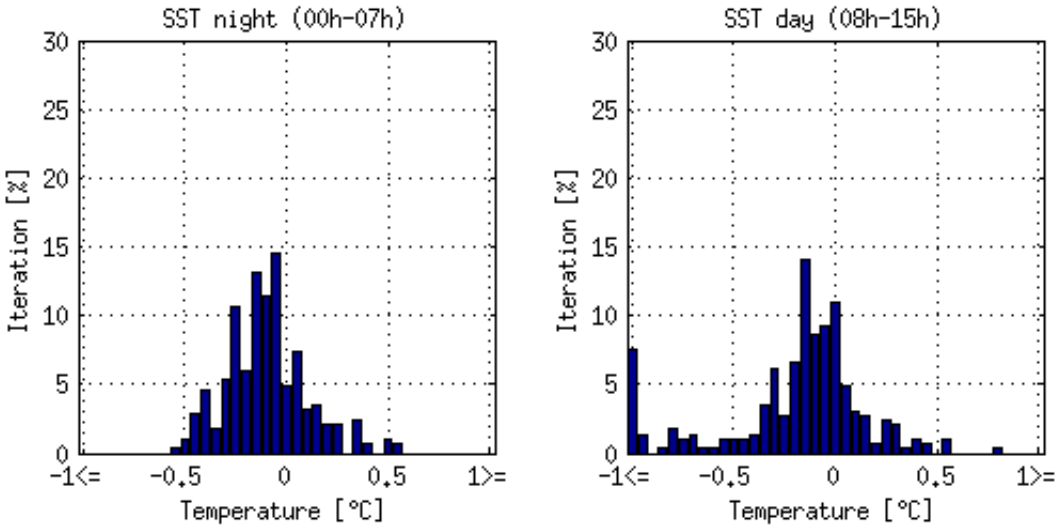


**Figure 13: Distribution of temperature differences between measurements by Marisonde and by SVP-BTC drifting buoys [Marisonde minus SVP-BTC], at the same times, for buoys located nearby [within 6 miles separation distance] during (Right) daytime [08h-15h, 290 comparisons] and (Left) night-time [00h-07h, 282 comparisons].**

Comparing the data in the time domain, the results shown in Figure 14 suggest that the Marisonde sensors suffer from a greater inertia than the SVP-BTC.

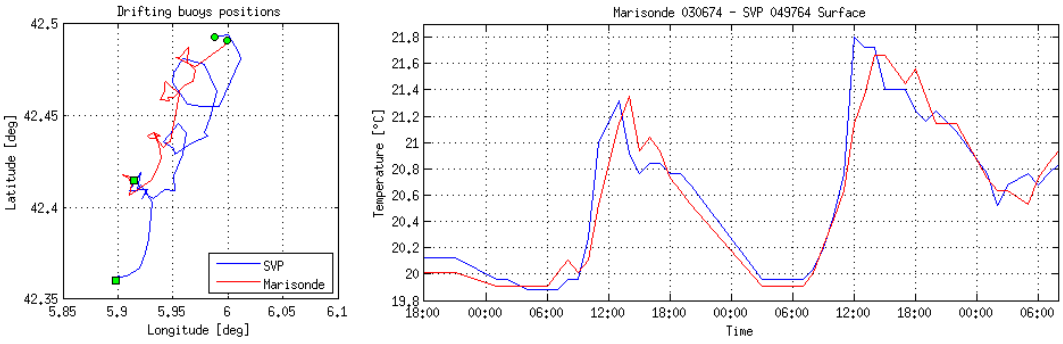


**Figure 14: Comparison of measurements by two drifting buoys [Marisonde WMO number 30674 and SVP-BTC WMO number 49764], located nearby [within 6 miles separation distance], between 04/11/2012 and 07/11/2012.**

At the sub-surface, the histograms feature differences that can sometimes exceed 1 K. It is hence interesting to try and understand better the differences at 25 m and 40 m depths. Chain uplifts as shown in Figure 15 are more frequent with SVP-BTC buoys than with Marisonde buoys. Over 11% of the time do such buoys suffer from chain uplifts greater than 8 m, against 4% of the time for Marisonde buoys. This is explained by the strings underneath the SVP-BTC buoys not being

fitted with deadweights, unlike the Marisonde strings. This implies that, in regions of strong gradients in temperature or currents, the data collected by both buoys necessarily differ.

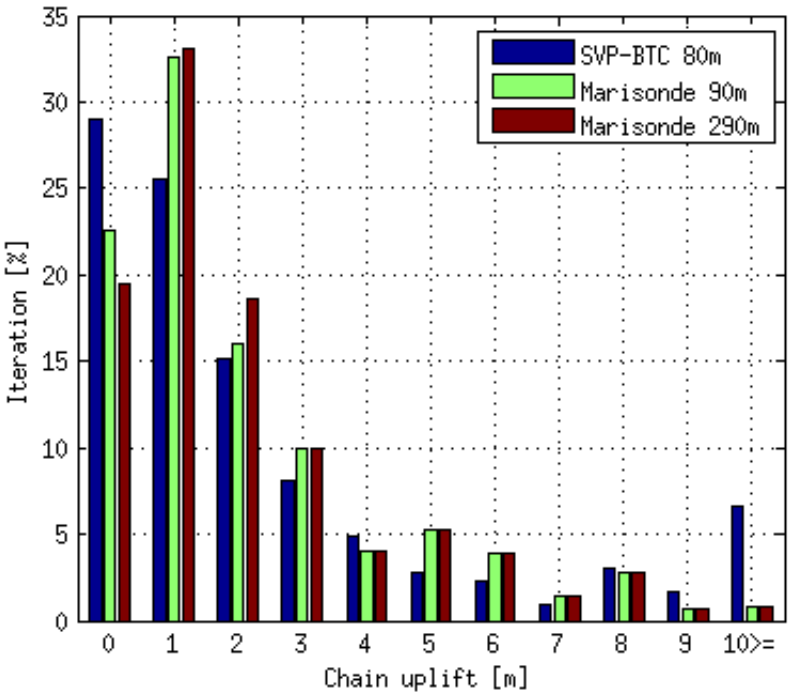


**Figure 15: Comparison of chain uplifting between SVP-BTC and Marisondes located nearby [at the same time, within 6 miles separation distance, amounting to 616 comparisons during HyMEX].**

Considering equivalent depths, Figure 16 shows differences after rejecting situations of 'large' (5 m or more) chain uplift events. Overall, the distributions are narrower than by considering all cases. Considering the level of highest potential gradient (25 m depth), the distributions are clearly different. Among all the data shown in Figure 12, 74% of the differences are within 0.5 K; after rejecting the large chain uplift events, this proportion is now 94% (note in particular how the bars counting errors greater than +/- 1 K have reduced in size). This clearly indicates that chain uplifts explain a large proportion of the differences seen initially.

However, at 40 m depth, differences larger than 1 K remain (representing 10%). The differences are also largely unchanged at 50 m and 75 m depths, with systematic effects (biases). These biases tend to suggest differing chain behaviors, with Marisonde strings more likely to be lifted only at the bottom, in contrast to SVP-BTC strings more likely to be lifted from their middle (around 40 m or 50 m).

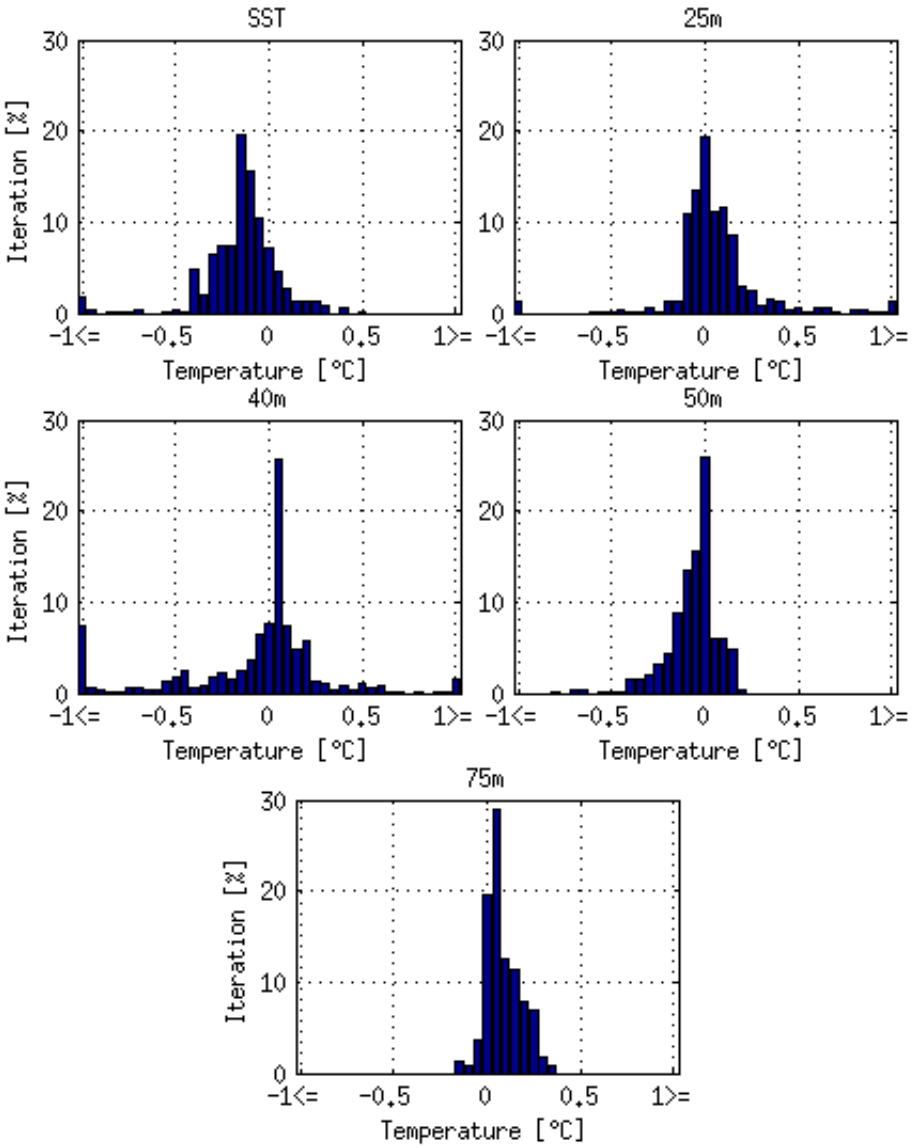


**Figure 16: Subsurface temperature differences at equivalent depths between measurements by Marisonde driting buoys and by SVP-BTC [Marisonde minus SVP-BTC], for nearby buoys [at the same time, within 6 miles separation distance], after removal of chain uplift events of 5 meters or more [509 comparisons during HyMEX].**

The differing chain behaviors shed light on another problem, inherent to all bathythermic string drifters: the necessity to model the chains. The realism of such models greatly influences the data quality of the resulting vertical profiles, especially for the SVP-BTC buoy which only measures hydrostatic pressure at the bottom of the string. Figure 17 presents the results of applying various models to SVP-BTC data: linear chain model, Météo-France chain model, and a novel model. Note

differences between models can reach up to 8 m. Météo-France's model assumes a vertical chain from the surface down to 13 m depth, and following a 2nd order polynomial thereunder, following equations of R. Thompson in « Displacement of Hydro-Acoustic modems by uniform horizontal currents » (2009). However, this model ignores the fixed chain length constraint. A novel model is proposed here, based on a similar algorithm, but adding the constraint that the chain cannot extend. For the Marisonde buoys, note it is preferable to use a linear model thanks to the presence of several hydrostatic pressure sensors. Figure 15 also suggests a rather linear behavior between such sensors.

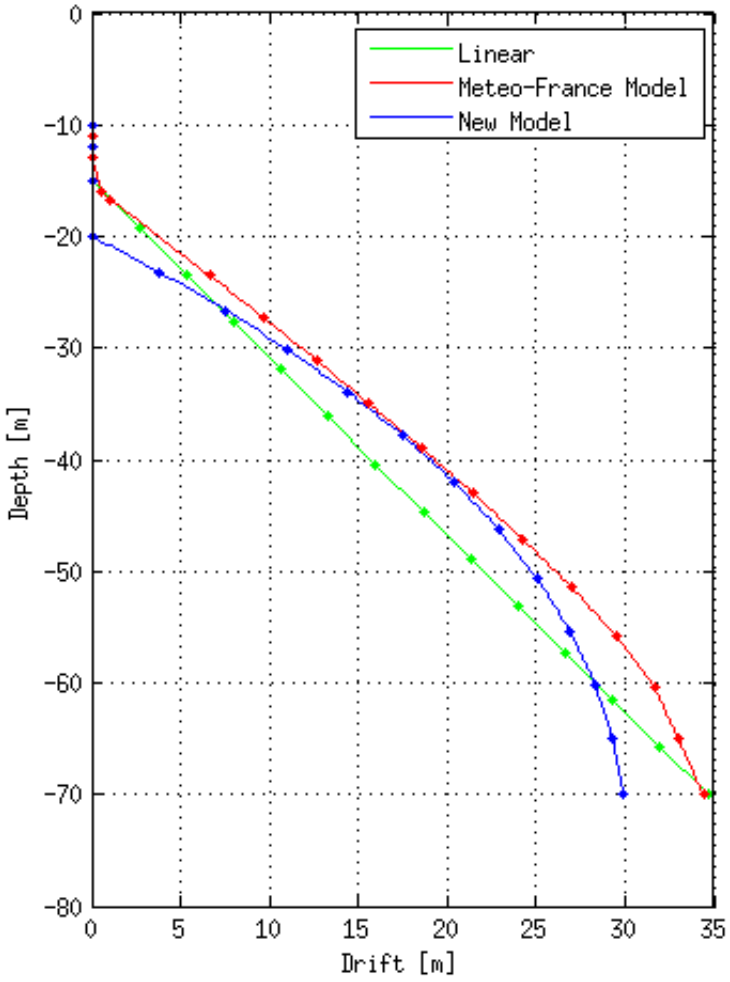


**Figure 17: Comparison of several chain depth models for a SVP-BTC drifting buoy.**

## Intercomparison: bathythermic string drifters compared with other platforms

This section aims at assessing the quality of the data from bathythermic strings. As shown above, because the chain model can influence the data quality, only the novel chain model is

considered thereafter. Comparisons are done with respect to thermosalinographs (TSG), Argo floats, and CTD. Note that because the T-FLEX platforms are rather recent, we found no sufficient amount of matching sub-surface comparisons with SVP-BTC and Marisonde. This section does not attempt to estimate uncertainty estimates from each observing system.

### Surface comparisons with TSG

During oceanographic campaigns EGEE and PIRATA-FR25, surface data collected by SVP-BTC and Marisonde buoys had been collected. These are compared with the TSG data from the ships that deployed these buoys. Table 4 indicates a good match between SVP-BTC and TSG. The biases are in line with specifications. The small negative biases with respect to TSG are consistent with known effects of ship-induced heating (Reverdin et al., 2008). However, the Marisonde data present a larger scatter with respect to the TSG data than the SVP-BTC data.

| Buoy type | Mission (Vessel) | Num | SST (TSG) | TIME (TSG) | SST (Buoy) | Time (Buoy) | Diff (Buoy-TSG) |
|---|---|---|---|---|---|---|---|
| SVP-BTC | FR25 (Thalassa) | 15951 | 28,5 | 22h32 | 28,48 | 23h00 | -0,02 |
| | | 15952 | 28,99 | 16h27 | 28,92 | 16h38 | -0,07 |
| | | 15953 | 29,29 | 17h46 | 29,22 | 17h49 | -0,07 |
| | EGEE (Atalante) | 57965 | 26,8 | 17h13 | 26,68 | 18h00 | -0,12 |
| | | 57966 | 28,6 | 12h46 | 28,52 | 13h00 | -0,08 |
| | | 66475 | 27,2 | 19h20 | 27,08 | 21h00 | -0,12 |
| | | | | | | | mean = -0,07 (std = 0,03) |
| Marisonde | EGEE (Atalante) | 15507 | 27,2 | 07h39 | 27,17 | 10h00 | -0,03 |
| | | 15508 | 27,1 | 19h08 | 27,15 | 21h00 | 0,05 |
| | | 15510 | 26,8 | 05h31 | 26,73 | 08h00 | -0,07 |
| | | 15511 | 25,8 | 10h50 | 25,92 | 13h00 | 0,12 |
| | | 15512 | 26,6 | 19h54 | 26,4 | 22h00 | -0,2 |
| | | 15515 | 27,3 | 20h52 | 26,91 | 23h00 | -0,39 |
| | | 15518 | 28,4 | 00h50 | 28,35 | 03h00 | -0,05 |
| | | 15521 | 28,6 | 06h30 | 28,53 | 08h00 | -0,07 |
| | | 15522 | 28 | 07h50 | 27,99 | 10h00 | -0,01 |
| | | 15527 | 25,4 | 02h02 | 25,19 | 04h00 | 0,09 |
| | | 15529 | 27,6 | 07h02 | 27,63 | 09h00 | 0,03 |
| | | 15534 | 24,6 | 00h30 | No Data | 04h00 | |
| | | | | | | | mean = -0,05 (std = 0,14) |

**Table 4: Surface temperature [°C] differences (Buoy thermistor string measurement) minus (Ship TSG measurement), when the buoys were deployed.**

In the remainder of the report, a collocation is applied, to find matching data pairs within 6 miles separation distance, and within 6 hours, considering the closest separation distance found in a given day.

For TSG, Figure 18 shows histograms of differences. The distributions are rather spread-out, with a negative bias for Marisondes. This may be the compound effect of TSG temperature overestimation and Marisonde surface temperature underestimation mentioned earlier.

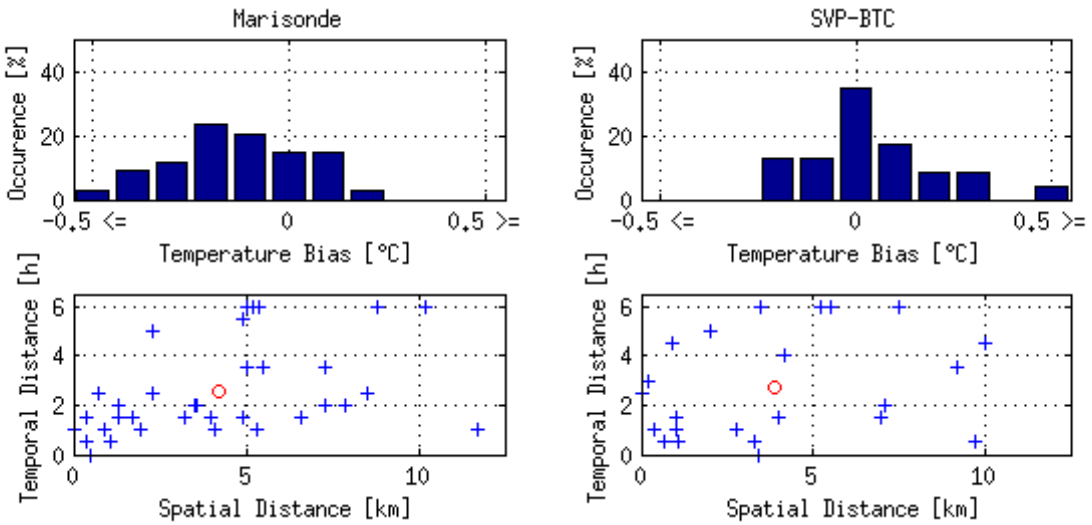


**Figure 18: (Top) Histogram of surface temperature differences between measurements by drifting buoys [23 SVP-BTC data points, 33 Marisonde data points] and thermosalinograph measurements from ships [buoys – TSG]. (Bottom) Spatio-temporal distribution of the data used for the comparison [red shows the average].**

## Comparison with Argo floats

In such comparison, there is no comparison of the surface data because floats tend to stop measuring a few meters below the surface. We consider matches that fall within bins of 5 m depth (there is no vertical interpolation). Also, we do not consider results that could be obtained by extrapolation of the Argo data from the subsurface to the surface.

Figure 19 shows histograms of differences at various depths. The distributions are rather normal with a slight positive bias for SVP-BTC and a slight negative bias for Marisonde. The biases are within 0.2 K.

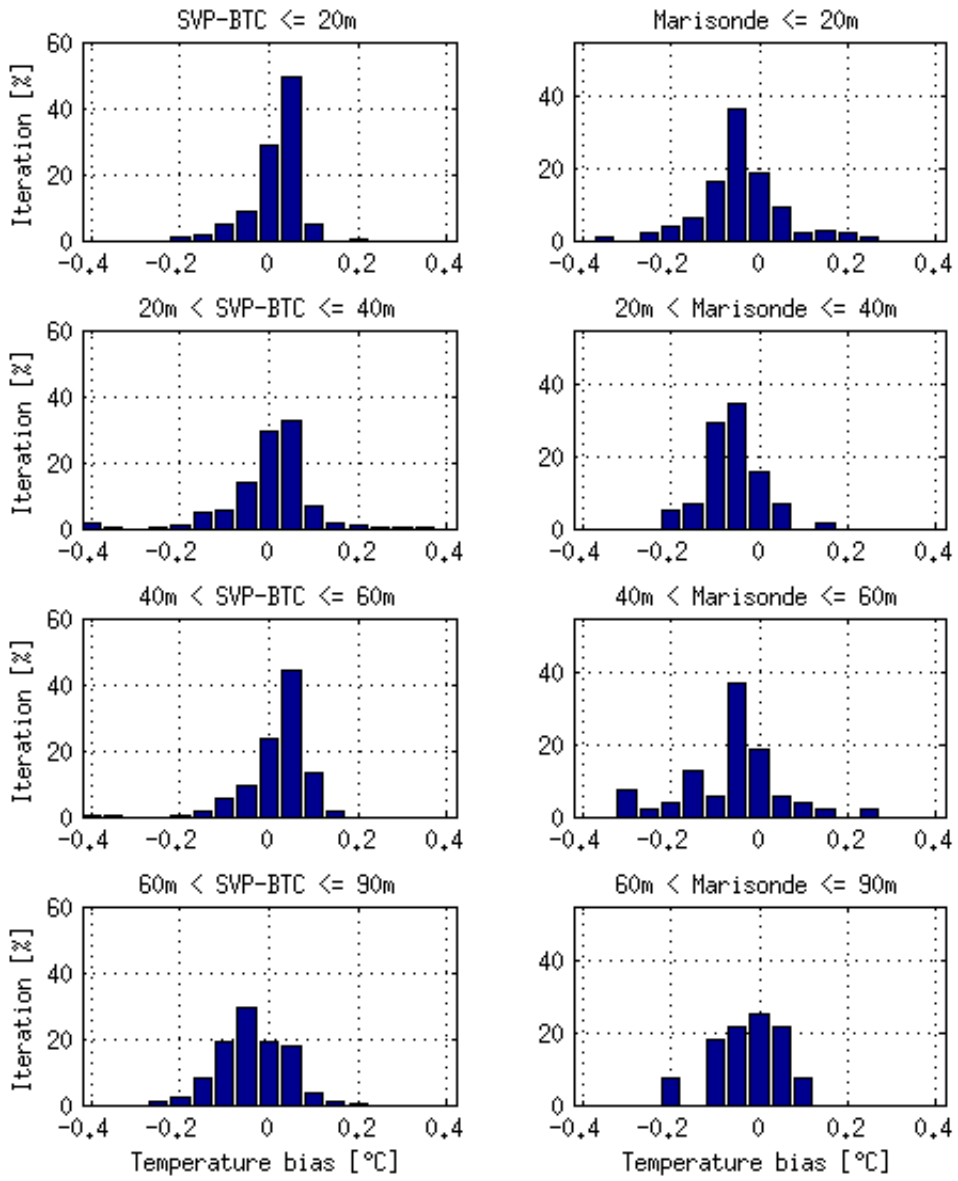


**Figure 19: Histograms, at various depths, of subsurface temperature differences between measurements by drifting buoys [(Left) 93 SVP-BTC profiles, (Right) 28 Marisonde profiles] and measurements by ARGO profiling floats [buoys – Argo].**

Considering the whole profile, Figure 20 enables to better see subsurface differences between Argo floats and collocated bathythermic string drifters. The results mentioned before are confirmed, with negative (positive) biases for Marisonde (SVP-BTC, respectively).

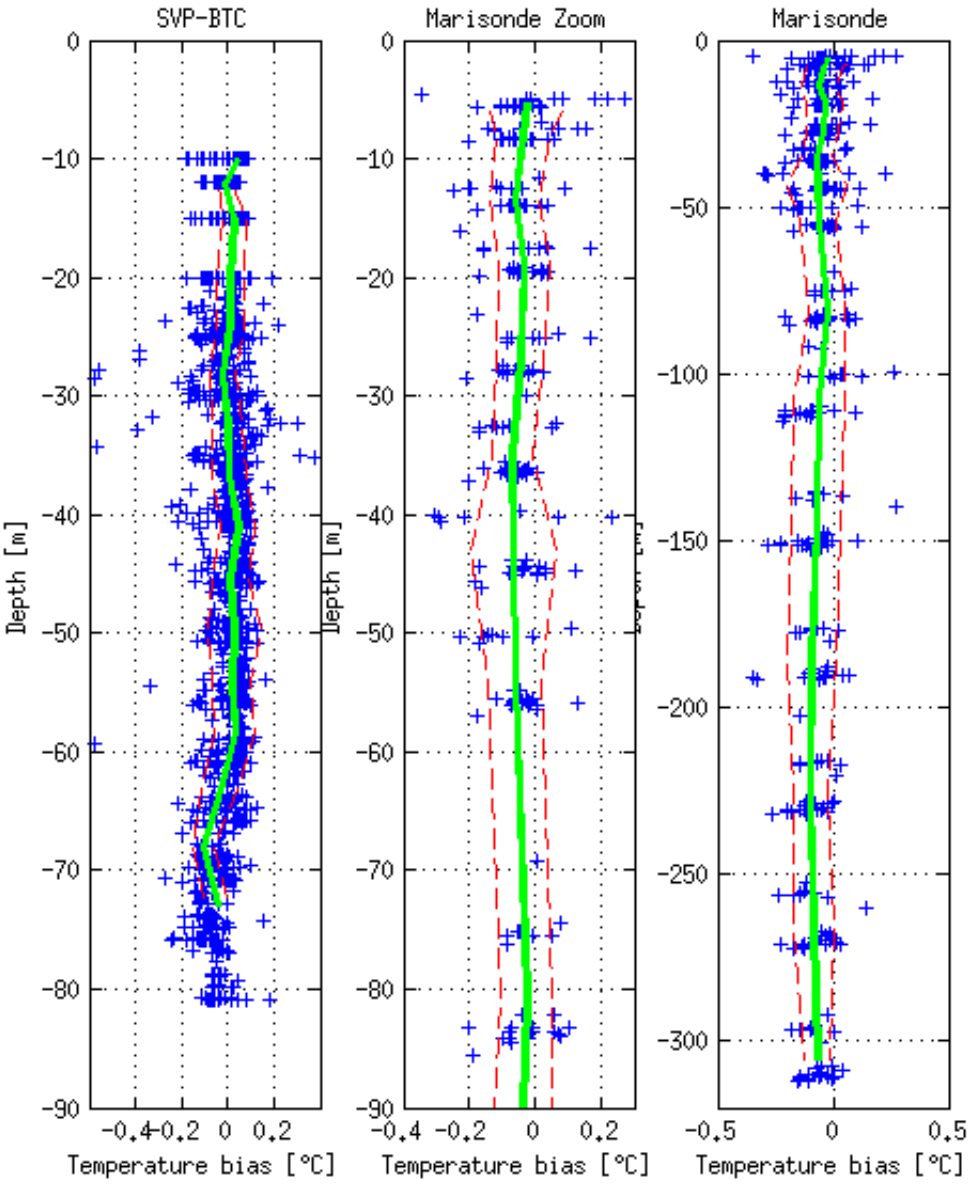


**Figure 20: Depth profiles of subsurface temperature differences between measurements by drifting buoys [(Left) 93 SVP-BTC profiles ; (Middle) 28 Marisonde profiles, zooming in on depths up to 90 m ; (Right) 28 Marisonde profiles down to 320 m depth] and measurements by ARGO profiling floats [buoys – Argo]. Green (red) line shows the mean (standard deviation, respectively) of the differences.**

The results shown in Figure 19 and Figure 20 consider all deployments. However, the Marisonde buoys found in the matching exercise are all located at low latitudes, whereas the SVP-BTC buoys are located at all latitudes.

Figure 21 shows SVB-BTC minus Argo differences by only considering high-latitude regions.

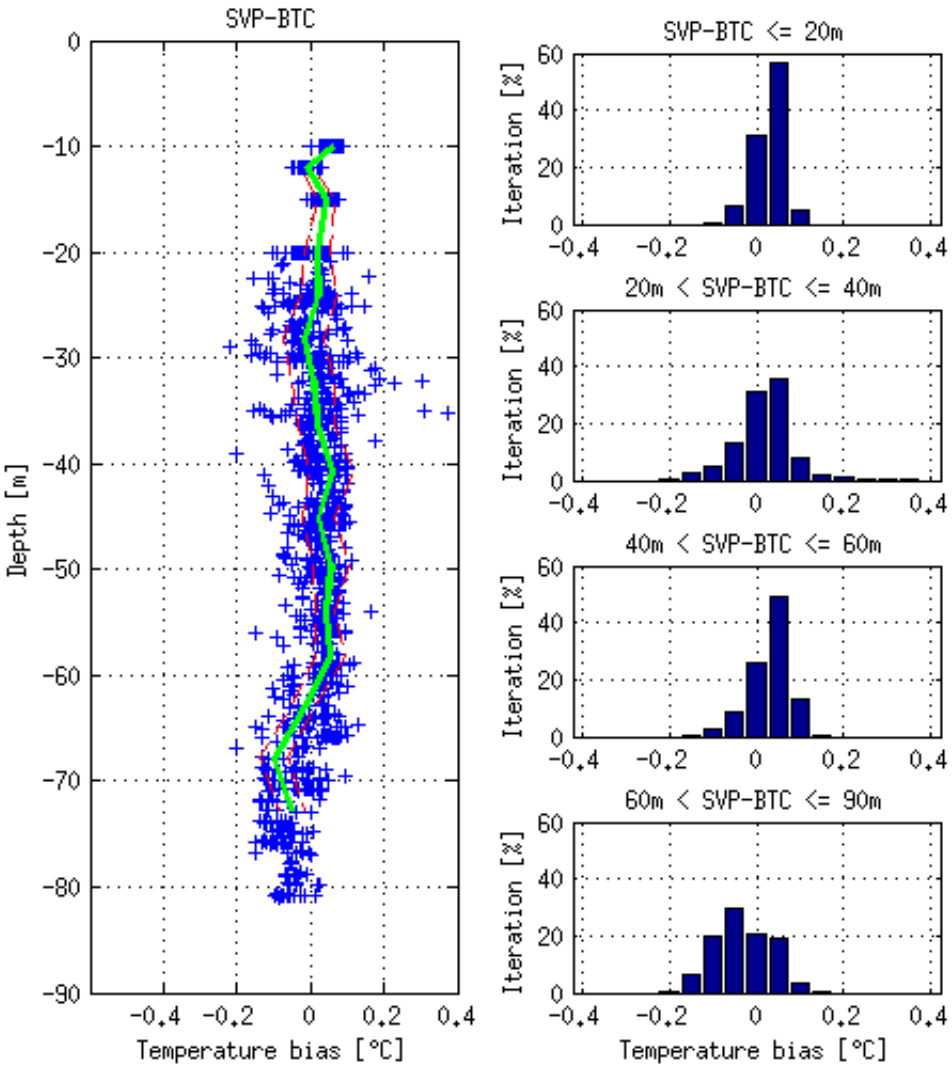


**Figure 21: (Left) Depth profile of subsurface temperature differences between measurements by SVP-BTC drifting buoys in high-latitude regions [80 profiles] and measurements by ARGO profiling floats [buoys – Argo]. Green line shows the mean difference. (Right) Histograms of those differences at several selected depth ranges.**

Conversely, Figure 22 shows results for low-latitude regions. Note differences with the earlier figure, and how the signs of the biases have changed at some depths.

This indicates that the biases found here are not significant, and that calibration of the SVP-BTC sensors can be further improved.

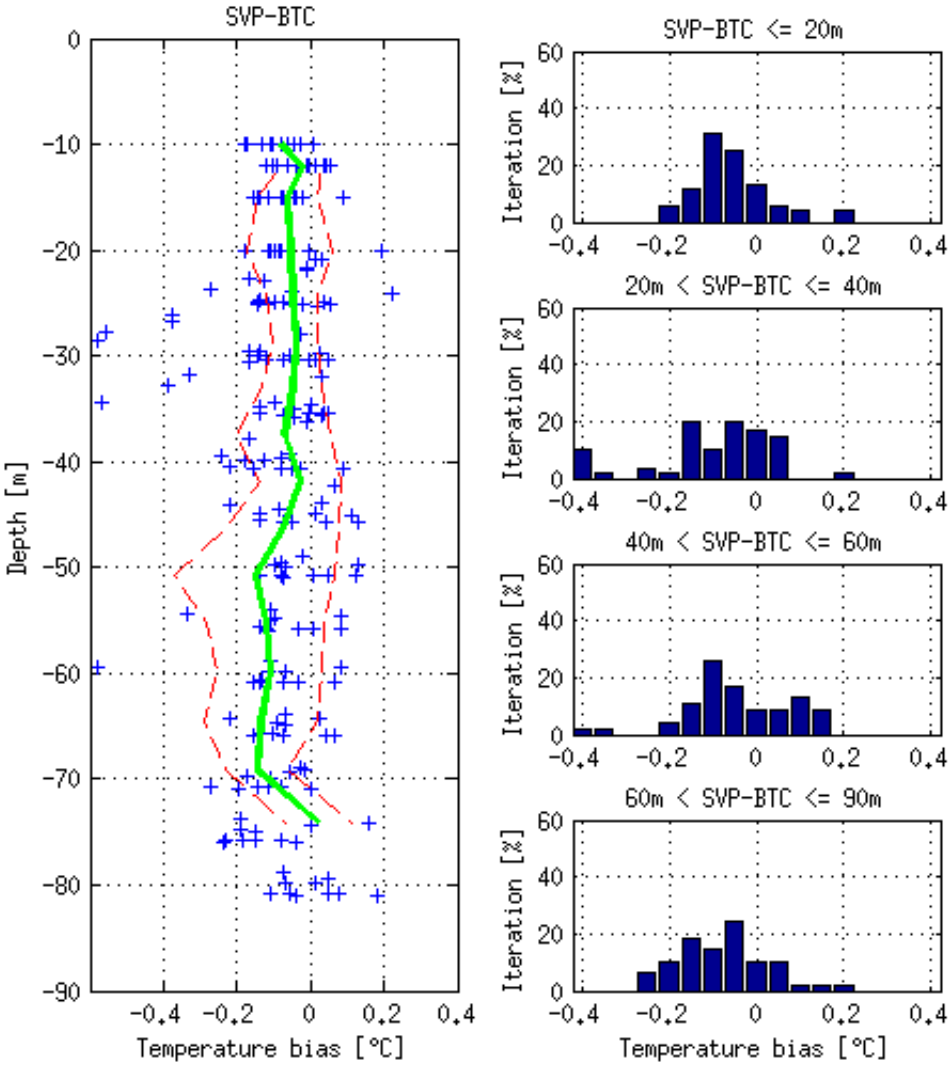


**Figure 22: (Left) Depth profile of subsurface temperature differences between measurements by SVP-BTC drifting buoys in low-latitude regions [13 profiles] and measurements by ARGO profiling floats [buoys – Argo]. Green line shows the mean difference. (Right) Histograms of those differences at several selected depth ranges.**

## Comparison with CTD

Figure 23 shows differences between SVP-BTC and collocated CTD. The differences tend to be negative. Note an insufficient number of collocations were found between Marisonde and CTD. Similar results are found as compared to Argo floats: the biases are within 0.2 K and are near-zero for the deepest levels. Note there is some uncertainty regarding the chain model, as the differences tend to be systematically negative near the middle of the chain (as was found for the comparison with Argo profiles).

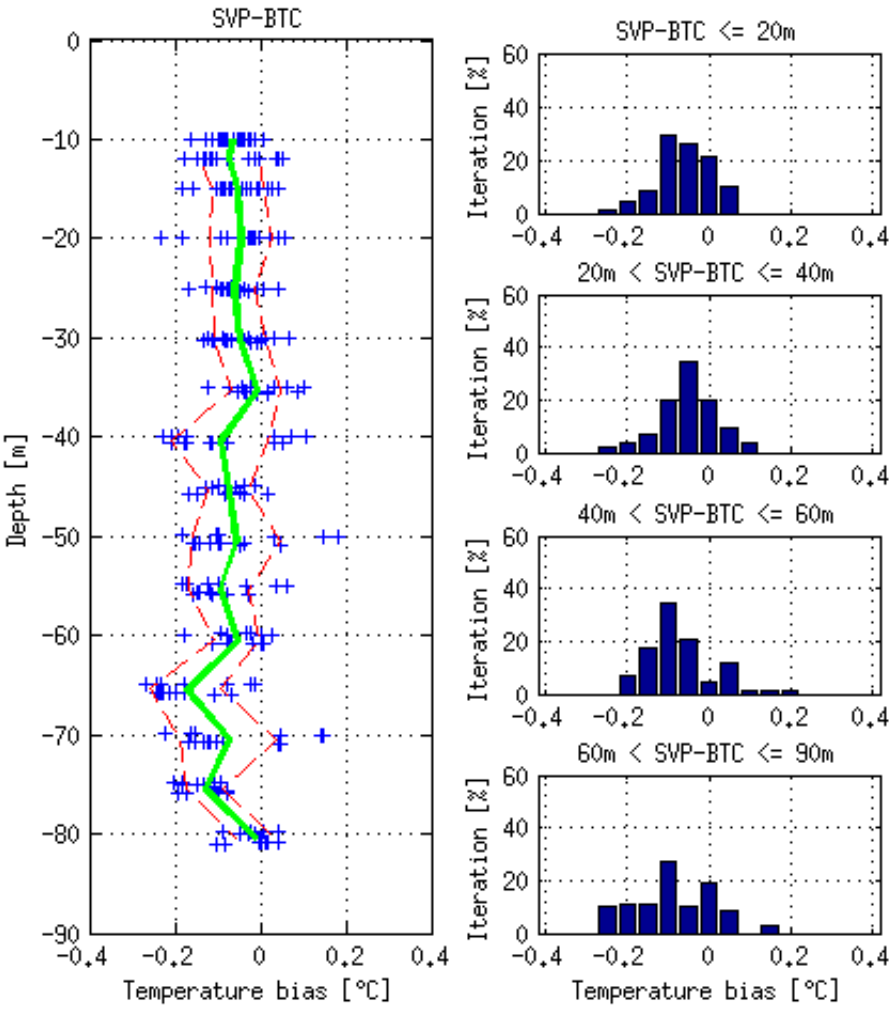


**Figure 23: (Left) Depth profile of subsurface temperature differences between measurements by SVP-BTC drifting buoys [19 profiles] and measurements by CTD [buoys – CTD]. Green line shows the mean difference. (Right) Histograms of those differences at several selected depth ranges.**

# IV. Discussion

## Limitations of the bathythermic string drifters

This report suggests the key limitation of bathythermic string drifters is the insufficient knowledge of the temperature measurement depth, especially when the chain is subject to large uplift events. Overall, these platforms suffer from an insufficient knowledge of the behavior of the string, whose depth is indeed only monitored at one or a few levels.

The chain models would need improving, and/or more hydrostatic pressure sensors would need to be placed along the string. The chain models used today are imperfect, and some even lack basic physical realism (the string has a finite length and cannot extend). The errors induced by these models are larger when subsurface currents are important, and when chains are not fitted with deadweights.

Clearly, a single sensor at the bottom of the string is insufficient.

In addition, the drag caused by the chain and its interaction with currents makes it difficult to exploit the data for current estimation. It is hence an illusion to hope to measure both currents and subsurface temperatures with such platforms, even though currents in the top layer may be inferred with a reduced accuracy.

Finally, these buoys require dedicated post-processing before analysis. The data in the CORIOLIS database are indeed generally raw data. These are contaminated by large biases when the string depth has not been recomputed to take into account actual air pressure and water density.

## Benefits of the bathythermic string drifters

Drifters with bathythermic strings are instruments that can collect high-quality sub-surface temperature profile data. Their resolution is half-way between Argo floats and moored buoys, but at a far higher temporal resolution. This high temporal resolution brings unique information to monitor ocean top layers.

Biases with Argo floats, CTD, and TSG, are generally smaller than 0.2 K, also in regions with strong vertical temperature gradients. When chain uplifts events are discarded, the biases are brought closer to zero.

## Future prospects

A novel chain model is proposed in the present report. Using this model, and looking for matching collocations with other instruments, satisfactory results are found.

The data used in the present study have been corrected for effects mentioned in the report, and are of greater quality than those found in the CORIOLIS database. The corrected data will be fed back to CORIOLIS, to improve the data record for future studies.

In spite of limitations outlined in this section, bathythermic string drifters should continue to

be used, taking into account the key recommendations of this report: 1) to monitor with more pressure sensors the depths of the measurements (as discussed already informally with manufacturer Marlin-Yug), 2) to place deadweights at the bottom of the strings whenever possible, and finally 3) to improve chain models.

# V. References and further reading


Blouch P., 2016. Recommended Iridium SBD dataformats for buoys. Météo-France.

Centurioni L.R and Niiler P.P., 2007. Drifting instrumented chains. New technical developments and applications. Science and Technology Workshop.

DeGasperi C., 2007. Major Lakes Continuous Temperature Study : Interim Progress Report.Department of Natural Resources and Parks.

du Penhoat Y., Reverdin G., Kartavtseff A., and Langlade M.-J., 1995. BODEGA surface drifter measurements in the Western Equatorial Pacific during COARE experiment (August 1992-July 1994). Notes Techniques Sciences de la Mer Océanographie Physique 11, available from http://horizon.documentation.ird.fr/exl-doc/pleins_textes/divers15-04/010022524.pdf (last accessed 29 March 2017)

Le Cann B. et al, 2005. Observed mean and mesoscale upper ocean circulation in the midlatitude northeast Atlantic. Journal of Geophysical Research.

Lumpkins R., 2005. Drifter observations of Hurricane Rita. Physical Oceanography Division. NOAA.

Mariette V., Verbeque V., Mouge P., and Deveaux M., 2002. A new concept for rapid assessment of oceanic environment. Operational oceanography implementation at the European and regional scales, pp. 289—297. Ed. Flemming N.C., Vallerga S., Pinardi N., Behrens H.W.A., Manzella G., Prandle D., and Stel J.H., Springer-Verlag.

Marlin-Yug, online : <http://www.marlin-yug.com/en/home/>.

Minnett P.J. and Hopkins T.S., 1991. Aspects of oceanographic Variability observed from thermistor chains on free-drifting buoys. Ocean Variability & Acoustic Propagation, 391-406.

McPhaden M.J., et al., 1991. A toga array of drifting thermistor chains in the western equatorial pacific ocean : october 1989- january 1990. PMEL, Seattle, Washington.

Motyzhev S., Lunev E. and Tolstosheev A. New Developments in the drifter Technologies. Marine Hydrophysical Institute.

Reverdin G. et al., 2008. XBT temperature errors during French research cruises (1999-2007).

Reverdin G., Gonella J. and Murail J.F., 1983. Etude comparative de dérive de bouées. Laboratoire d'Océanographie physique.

Reverdin G. and Kartavtseff, 1985. Bouées Focal, Recueil des trajectoires et séries temporelles. Museum National d'Histoire Naturelle.

Steele Michael, 2015. UpTempO buoys for Understanding and Prediction. University of Washington.

Timmermans M.-L., Melling H., Rainville L., 2006. Dynamics in the Deep Canada Basin, Arctic Ocean, Inferred by Thermistor Chain Time Series. American Meteorological Society.

Thompson S.R., 2009. Displacement of tethered hydro-acoustic modems by uniform horizontal currents. Monterey, California. Naval Postgraduate School.

Unesco, 1988. Guide to Drifting Data Buoys. Intergovernmental Oceanographic Commission. WMO.

UpTempO – Data Download – Level 2 QC Data Processing, online : <http://psc.apl.washington.edu/UpTempO/Level2_QC_doc.php>. Polar Science Center.

# Appendix I: Data found in the CORIOLIS database between 2006 and 2015

Remarks :

- Appellation : TS_DB [PR_TE : fixed point at 13 m ; PR_DR et PR_DB : fixed point at 0.5 m].
- Missing data are caused by drogue loss or failure of the hydrostatic pressure sensor. These is some delay between the time this happens and the actual end of the data transmission, so each time-series end has to be looked at with caution.
- Depths are affected by biases because the hydrostatic pressure sensor data are not used correctly (see this report).

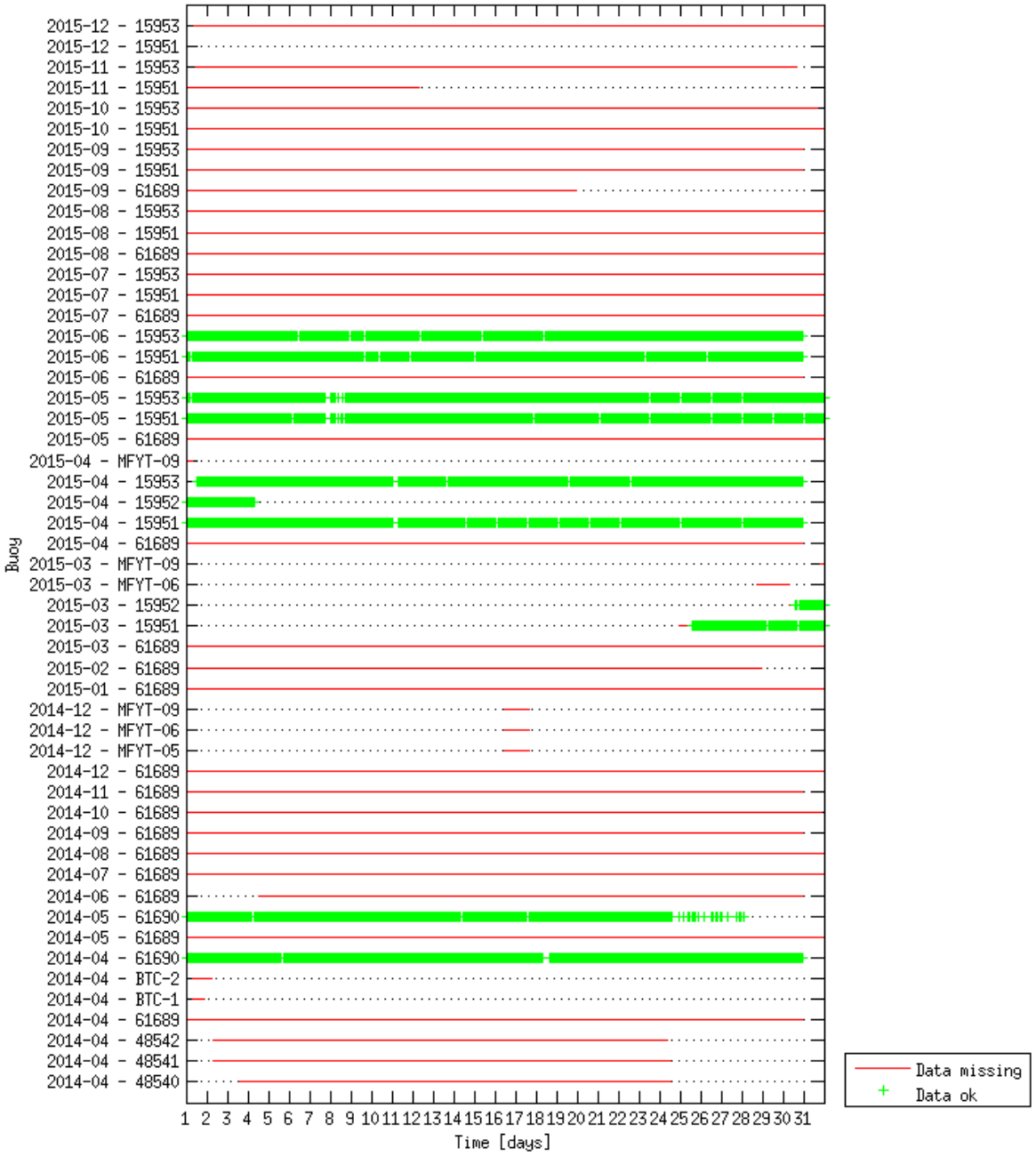
2015-12 - 15953
2015-12 - 15951
2015-11 - 15953
2015-11 - 15951
2015-10 - 15953
2015-10 - 15951
2015-09 - 15953
2015-09 - 15951
2015-09 - 61689
2015-08 - 15953
2015-08 - 15951
2015-08 - 61689
2015-07 - 15953
2015-07 - 15951
2015-07 - 61689
2015-06 - 15953
2015-06 - 15951
2015-06 - 61689
2015-05 - 15953
2015-05 - 15951
2015-05 - 61689
2015-04 - MFYT-09
2015-04 - 15953
2015-04 - 15952
2015-04 - 15951
2015-04 - 61689
2015-03 - MFYT-09
2015-03 - MFYT-06
2015-03 - 15952
2015-03 - 15951
2015-03 - 61689
2015-02 - 61689
2015-01 - 61689
2014-12 - MFYT-09
2014-12 - MFYT-06
2014-12 - MFYT-05
2014-12 - 61689
2014-11 - 61689
2014-10 - 61689
2014-09 - 61689
2014-08 - 61689
2014-07 - 61689
2014-06 - 61689
2014-05 - 61690
2014-05 - 61689
2014-04 - 61690
2014-04 - BTC-2
2014-04 - BTC-1
2014-04 - 61689
2014-04 - 48542
2014-04 - 48541
2014-04 - 48540
Buoy
1 2 3 4 5 6 7 8 9 10 11 12 13 14 15 16 17 18 19 20 21 22 23 24 25 26 27 28 29 30 31
Time [days]
Data missing
Data ok

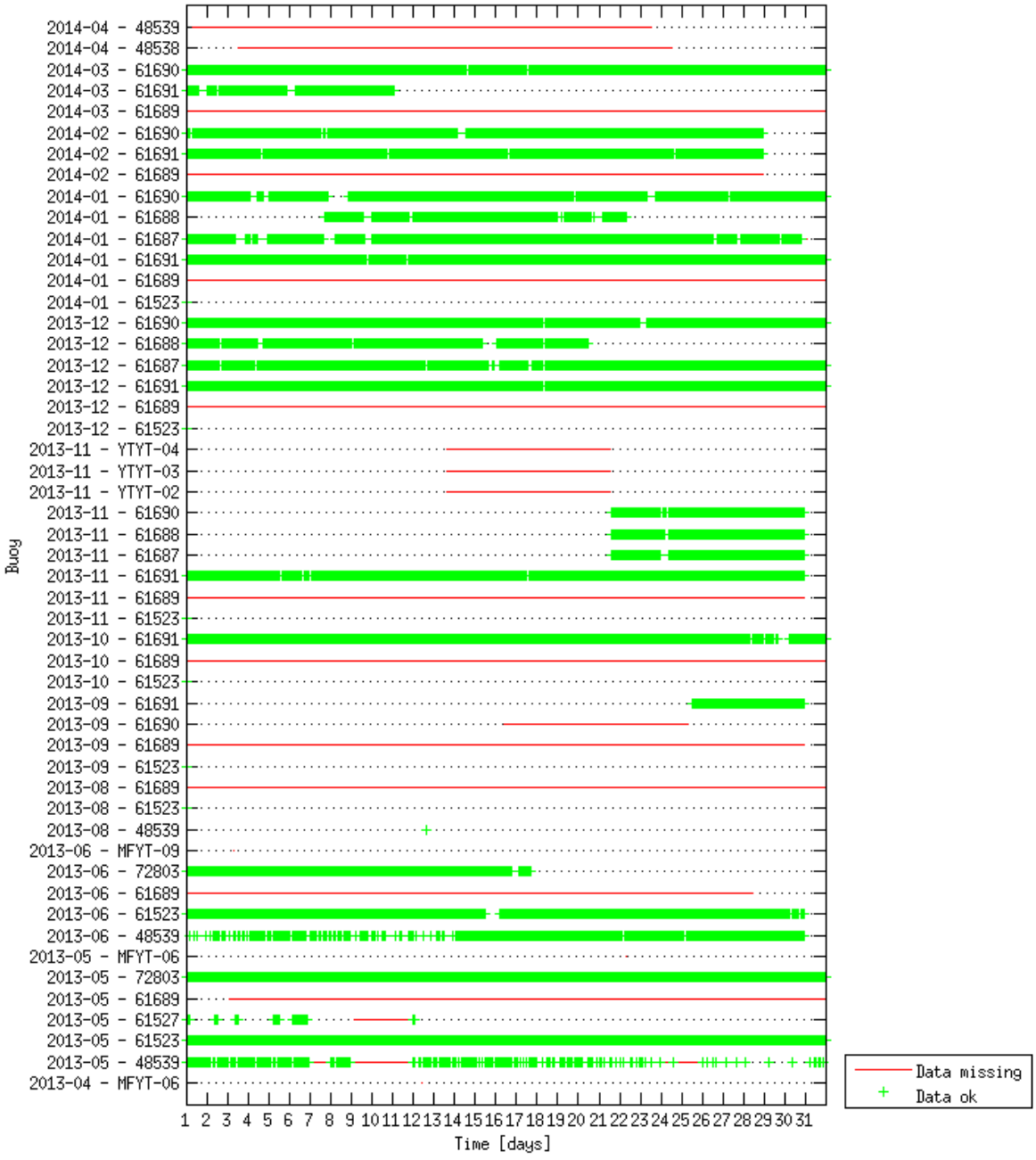
2014-04 - 48539
2014-04 - 48538
2014-03 - 61690
2014-03 - 61691
2014-03 - 61689
2014-02 - 61690
2014-02 - 61691
2014-02 - 61689
2014-01 - 61690
2014-01 - 61688
2014-01 - 61687
2014-01 - 61691
2014-01 - 61689
2014-01 - 61523
2013-12 - 61690
2013-12 - 61688
2013-12 - 61687
2013-12 - 61691
2013-12 - 61689
2013-12 - 61523
2013-11 - YTYT-04
2013-11 - YTYT-03
2013-11 - YTYT-02
2013-11 - 61690
2013-11 - 61688
2013-11 - 61687
2013-11 - 61691
2013-11 - 61689
2013-11 - 61523
2013-10 - 61691
2013-10 - 61689
2013-10 - 61523
2013-09 - 61691
2013-09 - 61690
2013-09 - 61689
2013-09 - 61523
2013-08 - 61689
2013-08 - 61523
2013-08 - 48539
2013-06 - MFYT-09
2013-06 - 72803
2013-06 - 61689
2013-06 - 61523
2013-06 - 48539
2013-05 - MFYT-06
2013-05 - 72803
2013-05 - 61689
2013-05 - 61527
2013-05 - 61523
2013-05 - 48539
2013-04 - MFYT-06
Buoy
1 2 3 4 5 6 7 8 9 10 11 12 13 14 15 16 17 18 19 20 21 22 23 24 25 26 27 28 29 30 31
Time [days]
Data missing
Data ok


2013-04 - MFYT-05
2013-04 - 72804
2013-04 - 72803
2013-04 - 72802
2013-04 - 61690
2013-04 - 61689
2013-04 - 61527
2013-04 - 61523
2013-04 - 48539
2013-03 - APYT-08
2013-03 - APYT-07
2013-03 - APYT-06
2013-03 - 72804
2013-03 - 72803
2013-03 - 72802
2013-03 - 61690
2013-03 - 61689
2013-03 - 61527
2013-03 - 61523
2013-03 - 61522
2013-03 - 48539
2013-02 - 61690
2013-02 - 61689
2013-02 - 61527
2013-02 - 61523
2013-02 - 61522
2013-02 - 48539
2013-01 - MFYT-08
2013-01 - MFYT-07
2013-01 - MFYT-06
2013-01 - MFYT-05
2013-01 - MFYT-04
2013-01 - MFYT-02
2013-01 - MFYT-01
2013-01 - 61690
2013-01 - 61689
2013-01 - 61527
2013-01 - 61523
2013-01 - 61522
2013-01 - 48539
2012-12 - YTYT-01
2012-12 - YTYT-00
2012-12 - 61690
2012-12 - 61689
2012-12 - 48539
2012-12 - 25596
2012-11 - YTYT-01
2012-11 - YTYT-00
2012-11 - 61786
2012-11 - 48539
2012-11 - 25597
Buoy
1 2 3 4 5 6 7 8 9 10 11 12 13 14 15 16 17 18 19 20 21 22 23 24 25 26 27 28 29 30 31
Time [days]
Data missing
Data ok

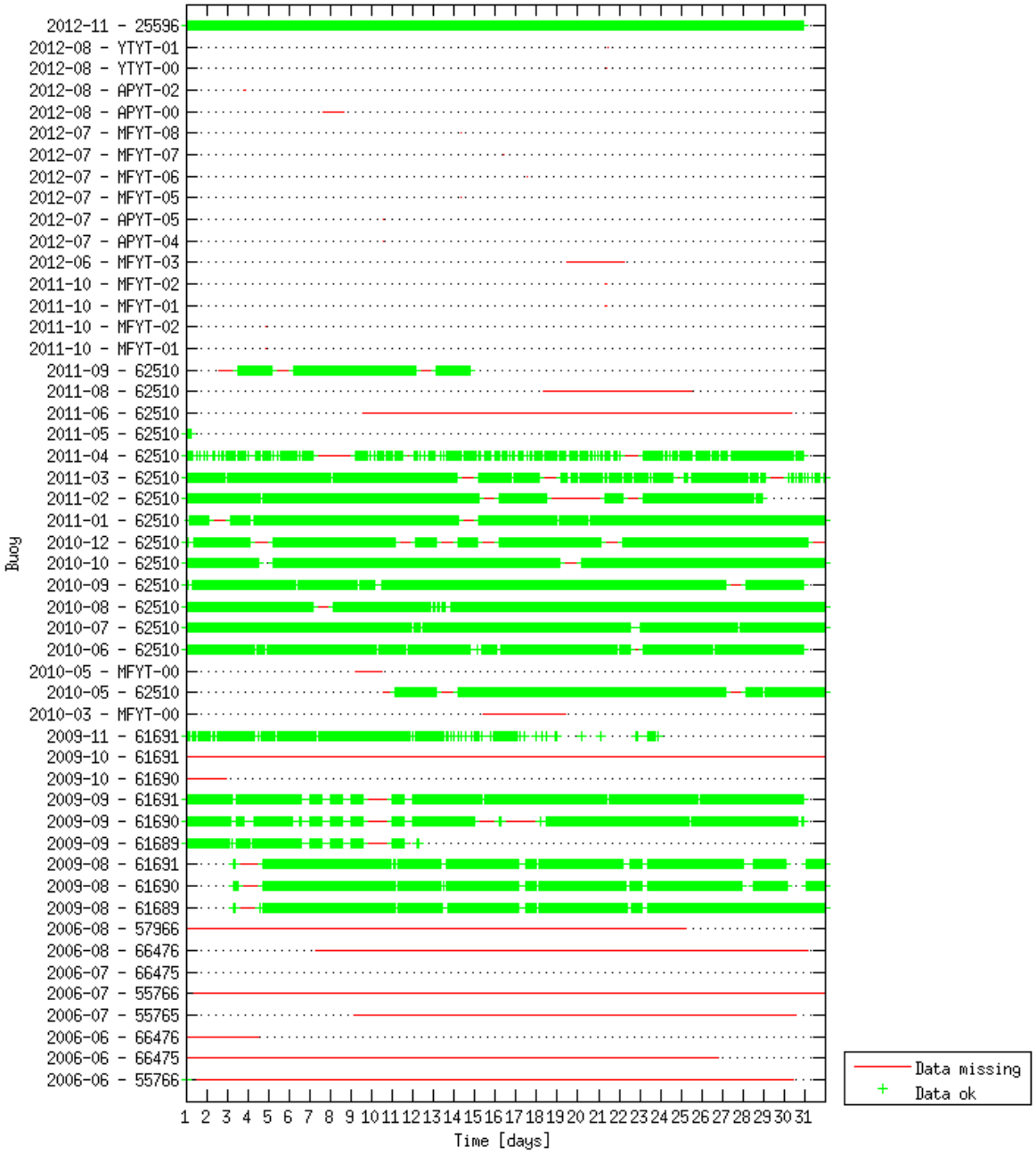
2012-11 - 25596
2012-08 - YTYT-01
2012-08 - YTYT-00
2012-08 - APYT-02
2012-08 - APYT-00
2012-07 - MFYT-08
2012-07 - MFYT-07
2012-07 - MFYT-06
2012-07 - MFYT-05
2012-07 - APYT-05
2012-07 - APYT-04
2012-06 - MFYT-03
2011-10 - MFYT-02
2011-10 - MFYT-01
2011-10 - MFYT-02
2011-10 - MFYT-01
2011-09 - 62510
2011-08 - 62510
2011-06 - 62510
2011-05 - 62510
2011-04 - 62510
2011-03 - 62510
2011-02 - 62510
2011-01 - 62510
2010-12 - 62510
2010-10 - 62510
2010-09 - 62510
2010-08 - 62510
2010-07 - 62510
2010-06 - 62510
2010-05 - MFYT-00
2010-05 - 62510
2010-03 - MFYT-00
2009-11 - 61691
2009-10 - 61691
2009-10 - 61690
2009-09 - 61691
2009-09 - 61690
2009-09 - 61689
2009-08 - 61691
2009-08 - 61690
2009-08 - 61689
2006-08 - 57966
2006-08 - 66476
2006-07 - 66475
2006-07 - 55766
2006-07 - 55765
2006-06 - 66476
2006-06 - 66475
2006-06 - 55766
Buoy
1 2 3 4 5 6 7 8 9 10 11 12 13 14 15 16 17 18 19 20 21 22 23 24 25 26 27 28 29 30 31
Time [days]
Data missing
Data ok

## Appendix II: Coefficients used in the Météo-France chain model for SVP-BTC

The polynomial equation to compute the depth (*H*, in meters) of each sensor of subsurface temperature, depending on the depth sensor value (*D*, in meters), is as follows:

$$H = C_0 + C_1 D + C_2 D^2$$

where $C_0$, $C_1$, and $C_2$ are coefficients of the polynomial equation (individual for each temperature sensor), indicated thereafter:

Coefficients to process the depth of the temperature sensor T2 (nominal depth=11 m):

C0= 11.0

C1= 0

C2= 0

Coefficients to process the depth of the temperature sensor T3 (nominal depth=13 m):

C0= 13.0

C1= 0

C2= 0

Coefficients to process the depth of the temperature sensor T4 (nominal depth=15 m):

C0= 15.84

C1= 5.091E-4

C2= 3.272E-5

Coefficients to process the depth of the temperature sensor T5 (nominal depth=20 m):

C0= 15.63

C1= 1.069E-2

C2= 6.871E-5

Coefficients to process the depth of the temperature sensor T6 (nominal depth=25 m):

C0= 15.34

C1= 2.506E-2

C2= 1.305E-3

Coefficients to process the depth of the temperature sensor T7 (nominal depth=30 m):

C0= 14.97

C1= 4.434E-2

C2= 1.878E-3

Coefficients to process the depth of the temperature sensor T8 (nominal depth=35 m):

C0= 14.50

C1= 6.948E-2

C2= 2.399E-3

Coefficients to process the depth of the temperature sensor T9 (nominal depth=40 m):

C0= 13.91

C1= 0.1017

C2= 2.856E-3

Coefficients to process the depth of the temperature sensor T10 (nominal depth=45 m):

C0= 13.17

C1= 0.1426

C2= 3.2319E-3

Coefficients to process the depth of the temperature sensor T11 (nominal depth=50 m):

C0= 12.24

C1= 0.1943

C2= 3.507E-3

Coefficients to process the depth of the temperature sensor T12 (nominal depth=55 m):

C0= 11.09

C1= 0.2599

C2= 3.649E-3

Coefficients to process the depth of the temperature sensor T13 (nominal depth=60 m):

C0= 9.64

C1= 0.3435

C2= 3.616E-3

Coefficients to process the depth of the temperature sensor T14 (nominal depth=65 m):

C0= 7.82

C1= 0.4514

C2= 3.341E-3

Coefficients to process the depth of the temperature sensor T15 (nominal depth=70 m):

C0= 5.52

C1= 0.5922

C2= 2.725E-3

Coefficients to process the depth of the temperature sensor T16 (nominal depth=75 m):

C0= 2.71

C1= 0.7767

C2= 1.629E-3

Coefficients to process the depth of the temperature sensor T17 (nominal depth=80 m):

C0= 0

C1= 1

C2= 0

## Appendix III: Novel chain model for SVP-BTC

The proposed polynomial equation to compute the depth (*H*, in meters) of each sensor of subsurface temperature, depending on the depth sensor value (*D*, in meters), is as follows:

$$H = C_0 + C_1(D - 20) + C_2(D - 20)^2 + C_3(D - 20)^3$$

where $C_0$, $C_1$, $C_2$, and $C_3$ are coefficients of the polynomial equation (individual for each temperature sensor), indicated thereafter:

Coefficients to process the depth of the temperature sensor T2 (nominal depth=10 m):

C0= 10.0

C1= 0

C2= 0

C3= 0

Coefficients to process the depth of the temperature sensor T3 (nominal depth=12 m):

C0= 12.0

C1= 0

C2= 0

C3= 0

Coefficients to process the depth of the temperature sensor T4 (nominal depth=15 m):

C0= 15.0

C1= 0

C2= 0

C3= 0

Coefficients to process the depth of the temperature sensor T5 (nominal depth=20 m):

C0= 20

C1= 0

C2= 0

C3= 0

Coefficients to process the depth of the temperature sensor T6 (nominal depth=25 m):

C0= 19,539

C1= 7,84E-2

C2= -1,6E-3

C3= 3,03E-5

Coefficients to process the depth of the temperature sensor T7 (nominal depth=30 m):

C0= 19,56

C1= 1.104E-1

C2= -1,6E-3

C3= 4,475E-5

Coefficients to process the depth of the temperature sensor T8 (nominal depth=35 m):

C0= 19,981

C1= 1,035E-1

C2= -2.166E-4

C3= 4,446E-5

Coefficients to process the depth of the temperature sensor T9 (nominal depth=40 m):

C0= 20.683

C1= 6,88E-2

C2= 2.3E-3

C3= 3,13E-5

Coefficients to process the depth of the temperature sensor T10 (nominal depth=45 m):

C0= 21,5035

C1= 2,2E-2

C2= 5,7E-3

C3= 8,131E-6

Coefficients to process the depth of the temperature sensor T11 (nominal depth=50 m):

C0= 22,231

C1= -1,59E-2

C2= 9,2E-2

C3= -2,083E-5

Coefficients to process the depth of the temperature sensor T12 (nominal depth=55 m):

C0= 22,605

C1= -1,75E-2

C2= 1,23E-2

C3= -4,974E-5

Coefficients to process the depth of the temperature sensor T13 (nominal depth=60 m):

C0= 22,347

C1= 4,93E-2

C2= 1,39E-2

C3= -7,106E-5

Coefficients to process the depth of the temperature sensor T14 (nominal depth=65 m):

C0= 21,261

C1= 2,153E-1

C2= 1,31E-2

C3= -7,631E-5

Coefficients to process the depth of the temperature sensor T15 (nominal depth=70 m):

C0= 19,516

C1= 4.893E-1

C2= 9,4E-3

C3= -5,928E-5

Coefficients to process the depth of the temperature sensor T16 (nominal depth=75 m):

C0= 18,265

C1= 8,093E-1

C2= 3,8E-3

C3= -2,498E-5

Coefficients to process the depth of the temperature sensor T17 (nominal depth=80 m):

C0= 20

C1= 1

C2= 0

C3= 0

# List of tables

# List of figures